

Spectroscopic binaries in a sample of ROSAT X-ray sources south of the Taurus molecular clouds¹

Guillermo Torres

Harvard-Smithsonian Center for Astrophysics, 60 Garden St., Cambridge, MA 02138, USA

Ralph Neuhäuser

Max-Planck-Institut für extraterrestrische Physik, D-85740 Garching, Germany

Eike W. Guenther

Thüringer Landessternwarte Tautenburg, Karl-Schwarzschild-Observatorium, Sternwarte 5,
07778 Tautenburg, Germany

ABSTRACT

We report the results of our radial-velocity monitoring of spectroscopic binary systems in a sample of X-ray sources from the ROSAT All Sky Survey south of the Taurus-Auriga star-forming region. The original sample of ~ 120 sources by Neuhäuser et al. was selected on the basis of their X-ray properties and the visual magnitude of the nearest optical counterpart, in such a way as to promote the inclusion of young objects. Roughly 20% of those sources have previously been confirmed to be very young. We focus here on the subset of the original sample that shows variable radial velocities (43 objects), a few of which have also been flagged previously as being young. New spectroscopic orbits are presented for 42 of those systems. Two of the binaries, RXJ0528.9+1046 and RXJ0529.3+1210, are indeed weak-lined T Tauri stars likely to be associated with the λ Ori region. Most of the other binaries are active objects of the RS CVn-type, including several W UMa and Algol systems. We detect a strong excess of short-period binaries compared to the field, and an unusually large fraction of double-lined systems. This, along with the overall high frequency of binaries out of the original sample of ~ 120 sources, can be understood as a selection effect since all these properties tend to favor the inclusion of the objects in a flux-limited X-ray survey such as this by making them brighter in X-rays. A short description of the physical properties of each binary is provided,

¹Some of the observations reported here were obtained with the Multiple Mirror Telescope, a joint facility of the Smithsonian Institution and the University of Arizona.

and a comparison with evolutionary tracks is made using the stellar density as a distance-independent measure of evolution. We rely for this on our new determinations of the effective temperature and projected rotational velocities of all visible components of the binaries. A number of the systems merit follow-up observations, including at least 4 confirmed or probable eclipsing binaries. One of these, RXJ0239.1–1028, consists of a pair of detached K dwarfs and may provide for a potentially important test of stellar evolution models once the absolute dimensions of the components are determined.

Subject headings: X-rays — stars: activity — stars: evolution — stars: pre-main sequence — binaries: spectroscopic

1. Introduction

With the launch of the ROSAT satellite and of its predecessor, the Einstein Observatory, a new dimension was added to the study of star-forming regions that has enabled us to probe the higher energies released by young stellar objects. Many X-ray sources associated with known classical T Tauri stars (cTTS) or weak-line T Tauri stars (wTTS) were detected by these space missions in molecular cloud regions that have traditionally been thought of as being the natural habitat of low-mass pre-main sequence (PMS) stars. Additional wTTS also in the immediate vicinity of the molecular gas were discovered, nearly doubling the known population of young stars of this kind.

But large numbers of similar objects have also turned up *around* these regions, far removed from the presently known cloud material. Systematic studies to search for young objects over large areas of the sky based on the (spatially unbiased) ROSAT All Sky Survey (RASS) have been carried out by Alcalá et al. (1995) in the Chamaeleon region, Wichmann et al. (1996) in the central region of the Taurus-Auriga association, Alcalá et al. (1996) in Orion, Krautter et al. (1997) in Lupus, Neuhäuser et al. (1995a; hereafter N95a) and Magazzù et al. (1997; hereafter M97) south of the Taurus-Auriga region, and Neuhäuser et al. (2000) in Corona Australis. These studies, mostly carried out at relatively low spectral resolution, have identified several hundred candidates that also have all the appearance of wTTS and their sheer numbers could have a significant impact on our understanding of issues such as the efficiency of the process of star formation. Follow-up studies with high spectral resolution to confirm the characteristic spectroscopic signatures of T Tauri stars among these candidates (late spectral type along with H α emission and strong Li I λ 6708 absorption) have also been performed, and a fraction of the objects (\sim 20-90%, depending

on the region; e.g., Covino et al. 1997, Wichmann et al. 1999, 2000) indeed seem to be very young (1-10 Myr). Kinematic studies to investigate the association of these objects with their parent clouds have provided important complementary information (N95a; Neuhäuser et al. 1997, hereafter N97; Alcalá et al. 2000; Wichmann et al. 2000).

Radial velocities for more than 100 X-ray sources in the region south of the Taurus-Auriga molecular clouds were reported by N95a and N97. In the course of that high-resolution spectroscopic survey we discovered several dozen spectroscopic binaries, three of which have been identified as pre-main sequence stars in earlier studies. Such systems are extremely interesting given that orbits have been determined for only about 40 PMS systems (Mathieu 1994; Melo et al. 2001), and the study of their properties can provide valuable insights into the process of star formation. In special cases these binaries allow one to determine the absolute masses of the components—the most basic property of a star—and can serve to test models of stellar evolution for young stars that are virtually unconstrained by the observations so far.

In this paper we present the results for the binary population of the sample of X-ray sources observed by N95a and N97, including new orbital solutions for 42 objects and a detailed discussion of each system. We also report determinations of the effective temperature and projected rotational velocity for all visible components, which aid in establishing the nature of these objects by comparison with recent stellar evolution models. As expected from their detection in X-rays by ROSAT, all of them are fairly active and this is reflected in some of their overall properties such as the orbital period distribution, which we compare with that for normal solar-type stars. Perhaps not surprisingly, the great majority of the systems are most likely of the RS CVn type, and a few belong to the Algol or W UMa class of interacting binaries. For at least two of our stars the spectroscopic and dynamical evidence suggests that they are bona-fide PMS objects, one of them possibly being as young as 1-2 Myr. These are potentially important systems that merit further study.

2. The sample

As described in more detail by N97, the objects in that study were originally selected on the basis of a combination of their X-ray properties as observed by ROSAT and also optical flux information (see Sterzik et al. 1995). Specifically, the X-ray hardness ratios HR1 and HR2 (N95a), the X-ray-to-optical flux ratios, and the visual magnitudes were used to sieve out from among the thousands of sources detected by ROSAT the objects that have properties similar to those of the known PMS stars, and which would therefore

also be more likely to be young (see also M97). The sample is effectively flux-limited, the limit being set by a maximum likelihood threshold to avoid confusion with the X-ray background (see Neuhäuser et al. 1995b). The 111 sources observed by N97 cover an area of several hundred square degrees south of the Taurus-Auriga star-forming region. Roughly 20% of them have been identified as being PMS stars on the basis of their spectral type and Li I $\lambda 6708$ absorption.

Of this sample of 111 stars, 40 objects are binaries for which we have determined the spectroscopic orbits. Ten additional sources in the same area were added after the publication of the N97 results, and were selected using somewhat relaxed criteria (see Zickgraf et al. 1998) and also proper motion information (Frink 1997, priv. comm.). Three of those are also binaries with orbits. A few systems flagged by N97 as having variable or possibly variable radial velocities have not been confirmed to vary with further observation, while others remain as possible binaries but require continued monitoring at much higher signal-to-noise.

X-ray and optical information for the 43 objects that turned out to be spectroscopic binaries are available from the studies by M97 and N97, and the relevant data for the present study are collected in Table 1 for easy reference. Additional measurements of the strength of the Li I $\lambda 6708$ line with higher spectral resolution than in M97 were obtained specifically for this project, and are also listed.

One of the objects, [30] RXJ0441.9+0537², is a member of a rare class of cool Algols (see, e.g., Popper 1992), and was reported earlier by Torres, Neuhäuser & Wichmann (1998). The remaining objects belong to a variety of categories ranging from normal main-sequence binaries to evolved systems of the RS CVn type, and are described in more detail below.

3. Spectroscopic observations and reductions

The observations of the ROSAT sources were obtained using a variety of telescopes and instruments, mostly at the Harvard-Smithsonian Center for Astrophysics (CfA), but occasionally also elsewhere.

At CfA we used three, nearly identical echelle spectrographs on the 1.5-m Wyeth

²The number in square brackets preceding the ROSAT designation here and throughout the paper is an internal reference number only (from Table 1), and is not intended for external use.

reflector at the Oak Ridge Observatory (Harvard, Massachusetts), the 1.5-m Tillinghast reflector at the F. L. Whipple Observatory (Mt. Hopkins, Arizona), and the Multiple Mirror Telescope (also on Mt. Hopkins) prior to its conversion to a monolithic 6.5-m mirror. A single echelle order centered at 5187 \AA was recorded using intensified photon-counting Reticon detectors, with a spectral window of 45 \AA . The resolving power of these observations is $\lambda/\Delta\lambda = 35,000$. The signal-to-noise ratios range from about 5 to 50 per resolution element. A total of 864 usable spectra of the stars identified as binaries in the N97 sample were obtained mostly from 1994 September to 2001 April.

Radial velocities for the single-lined objects were obtained from these spectra by cross-correlation using the IRAF³ task XCSAO (Kurtz & Mink 1998). Templates were selected from a large library of synthetic spectra based on model atmospheres by R. L. Kurucz⁴, computed for us by Jon Morse (Morse & Kurucz, in preparation; see also Nordström et al. 1994). These calculated spectra are available for a wide range of effective temperatures (T_{eff}), projected rotational velocities ($v \sin i$), surface gravities ($\log g$) and metallicities. The optimum template for each object was determined from extensive grids of correlations in temperature and rotational velocity (the two parameters that affect the radial velocities the most), for an adopted surface gravity and for solar metallicity. Constraints on the surface gravity on a star-by-star basis are discussed below.

For double-lined objects radial velocities were determined using TODCOR (Zucker & Mazeh 1994), a two-dimensional cross-correlation algorithm that uses two templates, one for each component of the binary. In a few cases the stars were found to be triple-lined, and in those situations we used an extension of TODCOR to three dimensions (Zucker, Torres & Mazeh 1995).

The precision of the radial-velocity measurements is typically about 0.5 km s^{-1} for single-lined spectra with sharp lines, but can be larger for fast rotators and for some of the double-lined objects, particularly when the secondary components are faint.

The zero-point of the CfA velocity system was monitored every night by obtaining twilight exposures at dusk and dawn, and applying systematic corrections for each observing run as described in more detail by Latham (1992). The accuracy of the CfA velocity system, which is within about 0.1 km s^{-1} of the reference frame defined by minor planets in the solar system, is documented in the previous citation and also by Stefanik et al. (1999).

³IRAF is distributed by the National Optical Astronomy Observatories, which is operated by the Association of Universities for Research in Astronomy, Inc., under contract with the National Science Foundation.

⁴Available at <http://cfaku5.harvard.edu>.

Occasional observations for a few of the stars were made also with an echelle spectrograph on the 2-m Alfred Jensch telescope in Tautenburg (Germany). We used the red grism covering the wavelength region from 5600 Å to 9600 Å, and with a 2'' slit the instrument yields a resolving power of about $\lambda/\Delta\lambda = 35,000$. The signal-to-noise ratios achieved range from 30 to about 100 per pixel.

Radial velocities from these spectra were measured using the IRAF routine FXCOR to cross-correlate each observed spectrum against a template. For the latter we used an observation of the late-type star HR 5777 (37 Lib, SpT K1 III-IV), with a mean radial velocity adopted from Murdoch, Hearnshaw & Clark (1993). Instrumental shifts were accounted for by monitoring the position of the telluric O₂ lines. Measurements of the Li I $\lambda 6708$ line were made on the best of the Tautenburg spectra, and are reported in Table 1.

The measured radial velocities of all our program stars in the heliocentric frame are listed in Table 2 (for the single-lined systems) and Table 3 (double-lined systems), available in full in electronic form.

4. Results

Stellar properties (T_{eff} , $v \sin i$) for the visible components of all the single-lined binaries were determined from the CfA spectra by performing cross-correlations against synthetic templates over a broad range of values in temperature and rotational velocity, and seeking to maximize the average correlation over all exposures of a given object. A similar procedure was followed for the double-lined objects using TODCOR. Because of the narrow wavelength region covered by our observations and the relatively few spectral lines available, the surface gravity and effective temperature are strongly correlated so that, for example, adopting lower gravities for our templates leads to cooler temperatures. Therefore, the value of $\log g$ was fixed for each component of each binary based on the nature of the star from an analysis of the orbit and other physical characteristics. The procedure was iterated until a consistent set of parameters was obtained.

An example of the $v \sin i$ and T_{eff} determinations for a single-lined binary is shown in Figure 1. The contours correspond to equal correlation value (averaged over all exposures), and the dots represent the result for each individual exposure for the object. For the double-lined binaries we first determined the $v \sin i$ for the two components, which has the largest effect, and then the temperatures for fixed values of the rotational velocity (see Figure 2). Iterations were carried out until convergence.

The effective temperatures, surface gravities, and projected rotational velocities determined from our CfA spectra are given separately for the single-lined binaries (SB1) in Table 2 and for the double-lined binaries (SB2) in Table 3. For the latter we list also the light ratio determined in the manner described by Zucker & Mazeh (1994). The light ratios (secondary/primary) range from 0.06 to 4.1, and although they correspond strictly to our spectral window (5165–5211 Å), they are quite close to the visual band. The estimated uncertainties in the temperatures and $v \sin i$ determinations are generally ~ 150 K and $1\text{--}3 \text{ km s}^{-1}$, respectively, although in some cases the errors may be considerably larger, as indicated by a colon (:) in Tables 2 and 3.

Spectral types for most of our stars have been published by M97 and are collected in Table 1. Those determinations have a quoted uncertainty of ± 1 or 2 subtypes, increasing to ± 3 subtypes for stars earlier than about G5, mostly due to differences in resolution between the standard library of stellar spectra that M97 adopted for reference (Jacoby, Hunter & Christian 1984) and the spectroscopic material they used (Alcalá 2001, priv. comm.). For the single-lined systems, where there is no confusion as to which component the spectral type corresponds, a useful comparison with the effective temperatures derived here is possible. In Figure 3 we have converted the spectral classifications by M97 to temperatures using the calibration by Gray (1992). There is systematic offset with our determinations of about 200 ± 30 K, our temperatures being hotter than those indicated by the spectral types, which suggests that one or both temperature scales could be in error. The difference depends, however, on the conversion table adopted. For example, we find the offset to be 270 ± 50 K using the table by Schmidt-Kaler (1982), and 340 ± 40 K if we adopt the table by de Jager & Nieuwenhuijzen (1987), always in the same direction. Direct temperature determinations to test our results based on synthetic spectra are unfortunately unavailable for these objects. The possibility of a systematic error in the spectral types was investigated by checking against independent spectral classifications by other authors. Only 6 of the stars listed by M97 that are either single-lined binaries or single stars (to avoid confusion in the double-lined systems) were found in studies of ROSAT X-ray sources by Zickgraf et al. (1998) and Li & Hu (1998). Three of these objects are among our program stars. In all six cases the spectral types by M97 are later than the other sources, by an average of 3.3 subtypes. Though admittedly a limited comparison, the difference is in the same sense and of the same magnitude as the discrepancy mentioned above, suggesting that the effect may be real. We therefore rely on our own temperature determinations in this paper for the analysis below.

Orbital solutions were obtained using standard non-linear least-squares techniques

(e.g., Press et al. 1992). For the double-lined systems the velocities of the primary and secondary components often have very different precision due to the different brightness or rotational velocity. For those cases the relative weights were determined iteratively as part of the solution, to achieve a reduced chi-square of unity.

Inspection of the residuals of the Tautenburg observations from preliminary orbits based on the more numerous CfA velocities revealed that the zero-point offset between the two systems was negligible. The two data sets were therefore merged.

The resulting orbital elements for the single-lined binaries in our sample are given in Table 4. They are the period (P , in days), the center-of-mass velocity (γ , km s^{-1}), the primary velocity semi-amplitude (K_A , km s^{-1}), the eccentricity (e), the longitude of periastron for the primary (ω , degrees), and the time of periastron passage for eccentric orbits or the time of maximum primary velocity for circular orbits (T , heliocentric Julian date). We list also the derived quantity $a_A \sin i$ (projected semimajor axis of the primary, in units of 10^6 km). The mass function $f(m)$ was also derived for each of the SB1 orbits. In Table 4 we list the cube root of the mass function ($f^{1/3}$, in units of M_\odot), which is the coefficient appearing in the expression $M_B \sin i = f^{1/3}(M_A + M_B)^{2/3}$ that is more convenient for evaluating the minimum mass of the secondary. The time span and number of observations are indicated as well, along with the rms residual from the fit.

For the double-lined binaries the elements are given in Table 5, and are the same as in Table 4 with the addition of the velocity semi-amplitude for the secondary (K_B). The derived quantities in this case are the mass ratio ($q \equiv M_B/M_A$), the relative semimajor axis ($a \sin i$, in units of R_\odot), and the minimum masses for both components ($M_A \sin^3 i$ and $M_B \sin^3 i$). Following the usual spectroscopic convention, the more massive star in the system is referred to as the primary (star A).

The orbital solutions for all systems (except for [30] RXJ0441.9+0537; see above) are represented graphically in Figure 4 together with the observations. The individual residuals from the fits are given in Table 2 and Table 3.

5. Comments on individual objects

The orbital solutions reported in §4 provide important dynamical information on our targets that, when combined with the measured effective temperatures and projected rotational velocities along with other clues, offers glimpses into the nature of each of these X-ray sources. This, in turn, allows us to understand some of the properties of this

population of binary stars.

In addition to comments on the particulars of some of our orbital solutions, in this section we offer our interpretation of each system using relatively simple hypotheses. For objects assumed to be on the main sequence we use estimates of the mass (M) and radius (R) based on our effective temperature determinations and standard tabulations of average stellar properties such as that by Gray (1992). For short-period systems, the orbits are typically circular due to the action of tidal forces, particularly in stars with convective envelopes. If that is the case then synchronization between the axial rotation of the components and the orbital motion is also a reasonable assumption, as is the alignment between the axes of each star and the axis of the orbit. The reason for this is that the timescales for these two processes are usually several orders of magnitude shorter than the timescale for circularization of the orbit, according to theory (see, e.g., Hut 1981).

With the hypothesis that tidal forces have produced the synchronization, alignment, and circularization of the orbit, relatively robust estimates of the surface gravity for the double-lined systems in our sample can be made based on the arguments that follow. The minimum masses in double-lined spectroscopic binaries are given by

$$M_{A,B} \sin^3 i = 1.0361 \times 10^{-1} P (K_A + K_B)^2 K_{B,A} \quad (1)$$

(in units of the solar mass when the elements are expressed in their customary units), where the notation $M_{A,B}$ refers here to the mass of component A or component B. The condition of synchronous rotation implies

$$v \sin i = \frac{50.615}{P} R \sin i, \quad (2)$$

where $v \sin i$ is the measured projected rotational velocity in units of km s^{-1} and P is the orbital period. Under the assumption of alignment the inclination of the rotation axis (i) is the same as that of the orbit. The general expression for the surface gravity, $\log g = 4.4377 + \log M - 2 \log R$, then leads to

$$\log g_{A,B} = 0.8616 - \log P + 2 \log(K_A + K_B) + \log K_{B,A} - 2 \log V_{A,B}^{\text{rot}} - \log \sin i, \quad (3)$$

in which we have abbreviated $v \sin i$ as V^{rot} . For moderate or large inclination angles the last term represents only a minor correction to the surface gravity, and can be ignored (e.g., $|\log \sin i| < 0.2$ dex for $i > 40^\circ$). When warranted, these estimates of $\log g$ have been used to improve our determination of the temperatures of the components, since the two parameters are correlated in the cross-correlation technique we use, as mentioned earlier.

Eq.(2) and the expression for the projected semi-major axis of the orbit of a double-lined binary (in units of the solar radius),

$$a \sin i = 1.9757 \times 10^{-2} P(K_A + K_B) , \quad (4)$$

allow one to estimate the radii of both stars in units of the separation ($R_{A,B}/a$), independently of the inclination angle since the $\sin i$ term cancels out. Whenever possible we have compared these with the expected relative sizes of the Roche lobes (which depend only on the mass ratio, q) to establish whether the system is detached. Semi-detached or contact configurations are usually a sign of mass transfer, which may contribute to the overall activity of the systems and their strong X-ray emission.

The relative radii also allow us to estimate the minimum inclination angle for eclipses to occur (i_{\min}), since that angle is simply $\cos i_{\min} = (R_A + R_B)/a$. Expressed in terms of observables, we have

$$\cos i_{\min} = \frac{V_A^{\text{rot}} + V_B^{\text{rot}}}{K_A + K_B} , \quad (5)$$

where again $V_{A,B}^{\text{rot}}$ and $K_{A,B}$ are in their customary units. Confirmation of eclipses in some of our systems would of course provide a wealth of other information, most importantly the knowledge of the absolute radii and masses. Very little (if any) precise photometry is available for our targets because they are relatively faint, but whenever available we have used the information in the HIPPARCOS Catalogue or the Tycho-1 Catalogue (ESA 1997) to support our interpretation.

As seen below, most of our systems prove to be evolved (post-main sequence) and have overall properties that support their classification as RS CVn-type systems. The great majority show very weak or no Li I $\lambda 6708$ absorption in their spectra (Table 1). In a few cases, though, the strength of the Lithium line is strong enough that an alternate interpretation is possible, namely, that the objects are young and are perhaps still in the pre-main sequence phase. We discuss this evidence in more detail in §6.1 and §6.2. The nature of some of the stars remains ambiguous, and follow-up observations would be useful to improve our understanding in those cases. Summaries for each system follow.

[1] **RXJ0209.1–1536.** The secondary star in this short-period SB2 system is relatively faint ($L_B/L_A = 0.19$), and its parameters are somewhat uncertain. The assumption of synchronization for the primary leads to a minimum radius of $R_A \sin i = 0.67 R_{\odot}$, from eq.(2). A normal radius of $0.79 R_{\odot}$ for a main sequence star of the measured temperature then gives $i \sim 58^{\circ}$. However, this implies a mass for this star of only $0.30 M_{\odot}$, which seems too small for a K0-K1 dwarf. It is more likely that the star is larger and therefore evolved,

and that the corresponding inclination angle is smaller. From eq.(5) the condition for eclipses is $i_{\min} \approx 61^\circ$. The system is detached. The formal eccentricity of the orbit is barely significant ($e = 0.0184 \pm 0.0090$, a 2σ effect), and is probably not real considering that the period is only 0.83 days and that both stars are convective.

[2] **RXJ0210.4–1308SW**. Single-lined binary with a very short period and a circular orbit. If the primary has a normal radius of about $0.75 R_\odot$ for a main-sequence star of its temperature (spectral type K2), the equatorial rotational velocity would be very close to the value of 56 km s^{-1} that we measure for $v \sin i$. The orbit may thus be viewed nearly edge-on. In that case, if the primary mass is that of a normal dwarf ($\sim 0.76 M_\odot$), the secondary would be an M5 dwarf. Alternatively, the primary may be somewhat evolved, and the inclination angle lower. There is a hint of a rising trend in the velocity residuals from the circular orbit that needs to be confirmed. RXJ0210.4–1308SW is actually the fainter component of a visual pair. The brighter star (TYC 5283-1690-1) is $2''$ NE, and has a mean radial velocity near the center-of-mass velocity of the object described here (N97).

[3] **RXJ0212.3–1330**. With a period of 6.7 days and a circular orbit, the stars in this SB2 system are likely to be synchronized with the orbital motion. The secondary is very faint ($L_B/L_A = 0.09$), and its temperature and rotational velocity are more uncertain. The minimum mass for the primary from the spectroscopic orbit is consistent with that expected for a normal main-sequence star with the temperature we determine (spectral type \sim K2). Similarly for the secondary. This suggests that the system may be eclipsing, and if so, it is particularly interesting because both stars would be under a solar mass and the system is well detached. The entry in the Tycho catalogue (TYC 5283-876-1) indicates a scatter in the V_T passband of about 0.6 mag, although the object is relatively faint and the significance of this somewhat questionable in view of the relatively low precision for such objects. Photometry to confirm this hint is underway. The measured $v \sin i$ for the primary star is also in agreement with the value expected from synchronization.

[4] **RXJ0218.6–1004**. Double-lined binary with a relatively short period (also known as TYC 5282-68-1). The stars are expected to be synchronized, and the measured $v \sin i$ values inserted into eq.(3) imply $\log g$ values of 3.5 and 4.0 for the primary and secondary, respectively, which we have adopted for the templates. The primary must therefore be evolved. This is supported by the much lower temperature we derive for that component, which explains the fact that the light ratio is $L_B/L_A = 2.1$ despite a mass ratio close to unity. The projected radii are $R_A \sin i = 3.0 R_\odot$ and $R_B \sin i = 1.8 R_\odot$, and both stars are well within their Roche lobes. The size of the secondary implies that it too must be somewhat evolved. A typical mass for the temperature we measure for that component (spectral type late F) leads to an inclination angle of about 65° . The system is thus unlikely

to be eclipsing since $i_{\min} \approx 73^\circ$. Our orbital solution indicates a marginal eccentricity ($e = 0.0069 \pm 0.0028$), but this may simply be an artifact due to distortions in the velocities related to surface activity on one or both components.

[5] **RXJ0219.7–1026.** The circular orbit in this SB2 system with a relatively short period suggests the components’ rotation may be synchronized with the orbital motion. In that case, from the measured $v \sin i$ of the primary its minimum radius is $R_A \sin i = 5.2 R_\odot$. Given the temperature we determine for this star, which is 600 K cooler than the secondary, it must be a subgiant. From eq.(3) its surface gravity is $\log g_A = 3.0$, which is the value we used for the corresponding template. Based on the mass ratio this star is considerably smaller than its Roche lobe. Therefore the system is detached. Because of the fairly extreme light ratio ($L_B/L_A = 0.06$), the rotation of the secondary is uncertain, but definitely small. This is consistent with it being a dwarf, in agreement with its derived temperature. We have thus adopted $\log g_B = 4.5$ for its template. A typical mass for such a star ($M_B \sim 0.86 M_\odot$) then leads to an inclination angle of $i \sim 61^\circ$, and a primary mass of about $1.6 M_\odot$. The system is not eclipsing. A weak Li I $\lambda 6708$ absorption line was measured by M97 (presumably corresponding to the brighter primary), who considered it as a possible PMS system. The Li detection was confirmed by N95a and N97, but the evidence above seems to rule out the interpretation that it is very young (see also §6.2). An alternate designation for this star is TYC 5282-2210-1.

[6] **RXJ0239.1–1028.** Another double-lined binary with a short period and a circular orbit. The rotational velocities expected for main-sequence stars of the temperatures we determine (assuming radii of $\sim 0.7 R_\odot$) are very close to the values we measure, implying an almost edge-on orbit. The expected masses are also similar to the minimum masses we derive. Follow-up photometry by L. Marschall (Gettysburg College) has confirmed the eclipsing nature of this system. Both stars are of spectral type mid-K, and the light ratio is $L_B/L_A = 0.36$. Detached eclipsing binaries with relatively low-mass components such as these are not very common, making this an interesting system for accurate mass and radius determinations. Photometric and spectroscopic observations are being continued towards this goal.

[7] **RXJ0248.3–1117.** Also known as PPM 710125. The residuals from the circular orbit of this 1-day period SB1 system are slightly larger than expected. We see no sign of the secondary component. The temperature of the primary is solar-like. If we assume it is a main-sequence star with a radius similar to the Sun that is rotating synchronously with the orbit, the predicted equatorial rotational velocity is very similar to the observed $v \sin i$, implying an orbit viewed close to edge-on. From the mass function the secondary would then be an early M star ($M_B \sim 0.45 M_\odot$), which would explain why it is not detected

spectroscopically. If the assumption of a main-sequence primary holds, then the system is well detached and eclipses are possible for inclination angles larger than $i_{\min} \approx 70^\circ$.

[8] **RXJ0251.8–0203.** The hypothesis of synchronization in this SB2 system with a circular orbit and a relatively short period, along with the measured values of $v \sin i$ for both stars, lead to minimum radii of $R_A \sin i = 4.1 R_\odot$ and $R_B \sin i = 3.6 R_\odot$. These are clearly too large for the measured temperatures, and imply that the stars are late G-type subgiants rather than dwarfs. The surface gravities from eq.(3) are close to 3.0 and 3.1 for the primary and secondary, respectively. The configuration of the system is detached, and the minimum inclination angle for eclipses to occur would be about 64° . The evolved nature of the system is supported by the fact that the stars do not quite follow the normal mass-luminosity relation for dwarfs. The measured light ratio is $L_B/L_A = 0.71$, and from a mass ratio quite close to unity it would be expected to be considerably larger. N95a reported a very weak Li I $\lambda 6708$ absorption line (equivalent width $\sim 0.06 \text{ \AA}$).

[9] **RXJ0254.8–0709SE.** The physical parameters of the stars in this rather faint double-lined binary are somewhat uncertain. Based on grids of cross-correlations with a range of synthetic templates it is clear that both components are very cool and slowly rotating. Based on the dM3 classification by Neuhäuser et al. (1997) we adopt templates with a T_{eff} of 3750 K and a surface gravity appropriate for dwarfs. The mass ratio of $q = 0.577$ is, however, unusually low for a double-lined system composed of main-sequence stars. A normal mass-luminosity relation for dwarfs⁵ would imply a secondary so faint in the visible that its lines would not be seen in the spectrum (see, e.g., Carney et al. 1994). Yet the light ratio we measure is $L_B/L_A = 0.19$, which suggests that the stars are perhaps not both dwarfs. The $H\alpha$ emission measured by M97 is the strongest in our sample. From the small minimum masses eclipses are very unlikely. A visual companion about one magnitude fainter is located approximately $6''$ NW (M97).

[10] **RXJ0255.8–0750S.** Double-lined binary with a circular orbit and a 3.7-day period. The temperatures of both components correspond to a spectral type K4 or K5. The light ratio is $L_2/L_1 = 0.68$. Assuming typical radii of $R \sim 0.7 R_\odot$, synchronous rotation implies equatorial rotational velocities of $9\text{-}10 \text{ km s}^{-1}$, marginally larger than our measured $v \sin i$ values. The minimum masses from the orbital solution are also slightly larger than the mass implied by the temperatures. Adopting $M \sim 0.7 M_\odot$ we obtain $i \sim 70^\circ$. From the measured $v \sin i$ values and eq.(5) the lower limit for eclipses is $i_{\min} \approx 84^\circ$, so that eclipses

⁵The standard M-L relation for dwarfs relates the mass to the *bolometric* luminosity. In this relation the exponent has a value of roughly 4. However, in the optical bands the relation is much steeper, as described by Carney et al. (1994), with exponents in the range 8-9, depending on the band.

are unlikely. The system is detached, and otherwise quite similar to [6] RXJ0239.1–1028. A faint visual companion is located 10'' north.

[11] **RXJ0300.9–1002**. This object (also known as HD 18775) was added to our program at a later stage. It is a double-lined binary with a short period and a circular orbit. From the measured values of $v \sin i$, and assuming synchronous rotation, the surface gravities for both stars are close to $\log g = 4.0$. They are likely to be slightly evolved. The object was observed by the HIPPARCOS mission (HIP 14050), and the parallax determination (distance = 80 pc) along with the total brightness of the pair ($V = 7.78$) and our light ratio ($L_B/L_A = 0.55$) allow the components to be placed on the H-R diagram. Both stars lie somewhat above the main sequence. However, the lack of Li I $\lambda 6708$ absorption (equivalent width $< 0.06 \text{ \AA}$) indicates it is not young.

The system is well detached, and eclipses are possible only for inclination angles in excess of 81° . Based on the minimum masses from our spectroscopic orbit and the estimated temperatures, the angle is almost certainly smaller than this. Eclipses are therefore ruled out, and this is consistent with the absence of photometric variability determined by HIPPARCOS mission.

[12] **RXJ0309.1+0324N**. This SB2 has a close visual companion approximately 2'' to the south that contaminates the spectrum of the main target under typical observing conditions. Thus our spectra are usually triple-lined. To handle this case we have employed a three-dimensional cross-correlation technique (see Zucker, Torres & Mazeh 1995), which is simply an extension of the TODCOR algorithm to three dimensions.

The orbital period of RXJ0309.1+0324N (0.455 days) is the shortest in our sample, and is the reason for the very large rotation rates of the components. The radial velocity precision is degraded because of this, and the physical parameters of the secondary star are more uncertain because in addition this component is relatively faint ($L_B/L_A = 0.24$). The mass ratio of $q = 0.544$ is unusually low for these to be normal stars: a standard mass-luminosity relation for dwarfs would imply a light ratio in the visible much smaller than we observe (Carney et al. 1994). Synchronization and the measured projected rotational velocities for the primary and secondary lead to minimum radii of $1.06 R_\odot$ and $0.85 R_\odot$, respectively. Both stars are clearly filling their Roche lobes, if not exceeding them, making this a contact system possibly of the W UMa type. The mass ratio is typical for such systems, as are the temperatures we derive. The orbit is circular. From eq.(3) the surface gravities are $\log g = 4.0$, ignoring the small contribution from the unknown inclination. The minimum inclination angle for eclipses to occur is $\sim 27^\circ$. Since this angle leads to masses that are much too large for the measured temperatures, we infer that i is considerably larger, and thus the system must be eclipsing. The object is included in

the Tycho catalog as TYC 58-166-1. A fairly large scatter of about 0.8 mag in the V_T passband is listed for this star, perhaps consistent with eclipses, but the uncertainty in these measurements makes this evidence inconclusive. The visual companion has a mean velocity not far from the systemic velocity of our program star.

[13] **RXJ0330.7+0306N**. Double-lined system (TYC 67-206-1). Synchronization and the measured values of $v \sin i$ imply that the primary star is approximately 1.4 times larger than the secondary, despite the similar temperatures. The light ratio is $L_B/L_A = 0.63$. If the secondary is normal, its temperature (spectral type G9) leads to a mass of $M_B = 0.86 M_\odot$, from which the primary would be $0.92 M_\odot$. The inclination angle is then $\sim 47^\circ$. The resulting radii ($1.45 R_\odot$ and $1.05 R_\odot$) are both larger than normal for dwarfs, and may indicate some degree of evolution. The system is detached, and does not eclipse ($i_{\min} \approx 67^\circ$). A faint visual companion is located some $30''$ south.

[14] **RXJ0339.6+0624**. The lower temperature for the primary compared to the secondary in this SB2 system strongly suggests that it is an evolved star. The measured $v \sin i$ of the primary along with the assumption of synchronous rotation, supported by the short period and circular orbit, indicate $\log g_A = 2.27 - \log \sin i$. Because the minimum masses are small, the inclination angle is also likely to be small so that its contribution to the predicted value of the surface gravity may be significant. If we make the simplest assumption that the secondary is a normal main-sequence star, its temperature corresponds to a mass of $1.17 M_\odot$ (spectral type F9), and the implied inclination angle is just under 15° . The resulting primary surface gravity is then approximately $\log g_A = 2.9$. Independently of the assumption on the secondary, the primary star appears to be large enough to fill its Roche lobe, indicating mass transfer. With a radius typical for an F9 dwarf, the secondary would be much smaller than its critical surface. A consistent picture then emerges of a semi-detached Algol-type binary in which the mass gainer is not as hot as in the “classical” Algols, and the mass transfer is probably still in the early stages such that the mass ratio has not yet reversed to become as extreme as in those systems. RXJ0339.6+0624 is unlikely to be eclipsing since the lower limit on i for this to be possible is $i_{\min} \approx 61^\circ$. The light ratio in this system is $L_B/L_A = 0.60$. M97 measured weak Li I $\lambda 6708$ absorption, but their suggestion of a possible PMS nature is not confirmed by the dynamical evidence presented above. See also §6.2.

[15] **RXJ0340.3+1220**. From the very short period (0.555 days), the primary in this SB1 system cannot be a very large star. Assuming it is a main-sequence object, the effective temperature leads to a mass and a radius about 0.7 times that of the Sun, corresponding to spectral type K4. The predicted equatorial rotational velocity is then about 64 km s^{-1} , and our $v \sin i$ of 54 km s^{-1} leads to $i \sim 57^\circ$. The secondary mass derived from the mass

function is expected to be about $0.17 M_{\odot}$, corresponding roughly to an M4 star. With the implied mass ratio, $q \approx 0.24$, the system is well detached. Given the radii and separation of the stars, eclipses are ruled out.

[16] **RXJ0343.6+1039.** With a mass ratio close to unity and a light ratio $L_B/L_A = 4.0$, one or both stars in this SB2 must be evolved. The fact that the primary temperature is cooler than the secondary is also symptomatic. From eq.(3) and the measured values of $v \sin i$ the primary has a surface gravity about 0.6 dex lower than the secondary, and is probably an early K subgiant. The system is detached, and the minimum inclination angle that would allow eclipses to occur is about 68° . Based on the minimum masses, the inclination angle is certainly smaller than this, so the system cannot be eclipsing. If a normal main-sequence mass of $1.3 M_{\odot}$ is adopted for the secondary based on its T_{eff} , the resulting inclination angle is in fact $\sim 26^\circ$. The corresponding radius of the secondary comes out $R_B = 1.9 R_{\odot}$, which is a bit large for a main sequence star of this temperature (spectral type mid F). It too may be slightly evolved. The surface gravities we have adopted to derive the final temperatures are thus $\log g_A = 3.5$ and $\log g_B = 4.0$. The presence of weak Li absorption, presumably corresponding to the much brighter secondary, prompted M97 to suggest a possible PMS nature for the object. This seems unlikely (see also §6.2).

The residuals of the primary star from our orbital solution are somewhat larger than expected and show systematic patterns perhaps indicative of surface activity (spotting). This could possibly be related to the strong X-rays in the system. Though not listed in the HIPPARCOS catalog, the object is included in the Tycho catalog (TYC 660-825-1) and there are indications that it may be photometrically variable (scatter in $V_T \sim 0.6$ mag).

[17] **RXJ0350.2+0849.** Short-period SB2 system with a circular orbit. The lower temperature for the more massive primary is indicative of evolution, at least in that star, as is the fact that the secondary is somewhat brighter ($L_B/L_A = 1.22$) for a mass ratio under unity. This is confirmed by the minimum radius for the primary that we derive from the measured rotational velocity and the hypothesis of synchronization: $R_A \sin i = 3.1 R_{\odot}$. The secondary also appears larger than normal for a main sequence star of its temperature ($R_B \sin i = 1.2 R_{\odot}$, for SpT \sim G7), so it too must have evolved to some extent. The system is detached, although the primary is about 86% of the size of its critical equipotential surface. The minimum inclination angle for eclipses to occur is 63° , but given the relatively small minimum masses we derive, eclipses seem unlikely.

[18] **RXJ0400.0+0730.** The secondary in this double-lined system is extremely faint ($L_B/L_A = 0.10$), which affects the precision of the radial velocities of that star and also makes the determination of its temperature and rotational velocity considerably more uncertain than those of the primary. Nevertheless, it is clear that the secondary is of much

earlier spectral type (mid A?) than the more massive primary, which must therefore be evolved (early G-type giant or subgiant). Synchronization in the system is a reasonable assumption for the short period and circular orbit. This along with our measured value of $v \sin i$ for the primary leads to a minimum radius $R_A \sin i = 3 R_\odot$, which is much larger than normal for a star of its temperature, and is therefore consistent with it being evolved. The system is detached.

[19] **RXJ0402.5+0552.** If synchronization is assumed in this 8.2-day SB1, a normal radius for a star of its temperature leads to an equatorial velocity slightly under 6 km s^{-1} , which is lower than the measured value $v \sin i = 14 \text{ km s}^{-1}$. This would suggest that the radius is at least $2.3 R_\odot$, implying that the primary star is slightly evolved, perhaps being an early G-type subgiant. Accordingly, we adopted a surface gravity of $\log g = 4.0$. The formal orbital solution gives a small but perhaps significant eccentricity of $e = 0.029 \pm 0.010$ (2.9σ). Though this may appear to undermine the assumption that the rotation is synchronized with the mean orbital motion, it is still quite possible that the system is pseudo-synchronized (i.e., synchronized at periastron) if the eccentricity is real, and the picture above would still hold. Alternatively, the measured eccentricity could be due to velocity distortions related to the activity in the binary. Further observations are needed to confirm the significance of the non-zero eccentricity. The star is also known as TYC 79-729-1.

[20] **RXJ0403.5+0837.** Synchronous rotation of the primary in the short-period circular orbit of this SB1 implies a minimum radius of $R_A \sin i = 1.45 R_\odot$, based on our measured $v \sin i$. Since this is larger than normal for a mid-G type dwarf, as inferred from the temperature, we conclude that the star is slightly evolved, and we have adopted a lower surface gravity accordingly ($\log g = 4.0$).

[21] **RXJ0405.5+0324.** The stars in this double-lined system (TYC 76-713-1) are similar in brightness ($L_B/L_A = 1.11$), but the mass ratio is smaller than unity ($q = 0.80$), and once again the secondary (of spectral type mid F) is considerably hotter than the primary. This suggests that the latter star is evolved (late G or early K subgiant or giant). The rotational velocity of the secondary is small and somewhat uncertain. A typical mass of $1.44 M_\odot$ for a star of its temperature leads to an inclination angle of roughly 42° , and a primary mass near $1.8 M_\odot$. From the hypothesis of synchronization and the measured rotational velocities the surface gravity of the primary would be lower by $\Delta \log g \approx 0.6$ dex, and its radius would be $R_A \sim 6.7 R_\odot$. The system is detached, and a minimum inclination angle $i_{\min} \approx 75^\circ$ indicates no eclipses.

The rather long orbital period of this binary (14.2 days) and its marginal eccentricity ($e = 0.0102 \pm 0.0048$, 2.1σ) may cast some doubt on the validity of the assumption of

synchronization. The independent evidence (from q and L_B/L_A) that the primary is evolved implies, however, that this star is larger and has a deeper convective envelope than a normal dwarf. Tidal forces are therefore expected to be much stronger, and possibly enough to have synchronized the axial spin of each star to the orbital motion, as well as circularized the orbit despite the wider separation. Whether the formal eccentricity is real or simply related to surface activity should be checked with further observations.

[22] **RXJ0408.6+1017.** Single-lined binary similar to [20] RXJ0403.5+0837, and with nearly the same period. The minimum radius implied by the measured $v \sin i$ is $R_A \sin i = 1.42 R_\odot$, which is larger than expected for a star with a temperature slightly cooler than the Sun. Some evolution is likely, and a value of $\log g = 4.0$ is adopted.

[23] **RXJ0410.6+0608.** The measured projected rotational velocity of the primary is small but rather uncertain in this SB1. The temperature corresponds to a spectral type near K2 for a main-sequence star. Adopting a typical mass of $M_A \sim 0.76 M_\odot$, the secondary star would be of spectral type M3 or earlier. The possibility suggested by M97 that this is a PMS system, based on their detection of weak Li I $\lambda 6708$ absorption, seems unlikely.

[24] **RXJ0422.9+0141.** As in [16] RXJ0343.6+1039, the mass ratio in this double-lined system is close to unity but the secondary is much brighter than the primary ($L_B/L_A = 4.1$ at a mean wavelength of 5187 \AA), and is also hotter. The primary must be evolved, perhaps being an early K giant or subgiant. M97 reported weak Li I $\lambda 6708$ absorption in both components, and advanced the possibility that it might be a PMS system. N97, on the other hand, considered it to be a zero-age main sequence (ZAMS) system with an age of the order of 30 Myr, but based only on the temperature of the hotter secondary. From the properties discussed above, the PMS scenario can be ruled out, and a post-main sequence picture seems more likely. Further support for this is given in §6.2 by comparison with evolutionary tracks.

Using eq.(3) the difference in surface gravities is $\Delta \log g \approx 0.8$, the primary value being lower. The system is detached, and i_{\min} is about 70° . A normal main sequence mass for the secondary of $1.3 M_\odot$ corresponding to its measured temperature (mid F star) would imply an inclination angle close to 63° , which would make eclipses unlikely. With this inclination the sizes of the stars would be $R_A \sim 4.4 R_\odot$ and $R_B \sim 1.8 R_\odot$, and the primary mass would be $1.35 M_\odot$. The larger radius of the secondary compared to a normal F star would indicate that it too is somewhat evolved. The unusually large scatter of the primary velocities from the orbital fit may be a sign of surface activity in the form of spots. Overall this system is remarkably similar to [16] RXJ0343.6+1039, except perhaps for the higher inclination angle.

[25] **RXJ0427.8+0049.** Synchronization in this short period SB2 system with a circular orbit leads to minimum radii of $R_A \sin i = 2.0 R_\odot$ and $R_B \sin i = 1.4 R_\odot$. The value for the secondary is only slightly larger than normal for a late F or early G main-sequence star, but perhaps consistent if one accounts for the measurement errors in $v \sin i$. The primary, on the other hand, appears considerably larger than normal, and is likely to be evolved. An assumed mass of $1.1 M_\odot$ for the secondary based on its effective temperature leads to an inclination angle of about 69° , whereas the minimum angle for eclipses to occur is 75° . The system is well detached, and the light ratio is $L_B/L_A = 0.67$. Alternate designations are BD+00°760 and TYC 75-1529-1.

[26] **RXJ0429.9+0155.** Both stars in this long-period double-lined binary are slow rotators. The minimum masses seem large for main-sequence stars of the temperatures that we determine (SpT G9-K0). The stars are possibly evolved. The mass ratio is close to unity ($q \equiv M_B/M_A = 0.94$, and the light ratio is $L_B/L_A = 0.24$). The system is well detached, and is also known under its Tycho designation TYC 75-1-1.

[27] **RXJ0434.3+0226.** The temperature we determine for the primary in this very long period, eccentric single-lined binary corresponds to spectral type K2, if it is a main sequence star. In that case, the minimum mass of the secondary corresponds to spectral type M3. Little more can be said about the nature of the system from the dynamical information alone. M97 measured moderate Li I $\lambda 6708$ absorption and considered the object to be in the PMS phase. Our own measurements confirm the presence of Li, which is stronger than the nearby Ca I $\lambda 6718$ line. The classification was refined by Magazzù, Umana & Martín (1999), who listed it as a post-T Tauri star (PMS star with significant Li depletion). N97 reported a similar conclusion, estimating the age to be less than ~ 30 Myr. Consequently, the surface gravity we have adopted ($\log g = 4.0$) is slightly lower than that corresponding to a normal main-sequence star.

[28] **RXJ0435.5+0455.** Similar to previous system, with a K0 primary (if on the main sequence) and a minimum secondary mass corresponding roughly to an M4 star. Tycho designation TYC 90-936-1.

[29] **RXJ0441.1+1132.** The secondary in this short-period SB2 is very faint ($L_B/L_A = 0.07$), and its temperature and projected rotational velocity are very uncertain. The assumption of synchronization and a normal radius for a main-sequence star with the temperature we determine for the primary lead to a rotational velocity for that star that is slightly lower than actually measured, but possibly consistent within the errors. The minimum mass for the primary from our spectroscopic orbit is also close to the typical value for that temperature, so that the data are consistent with a K0 primary in an orbit viewed nearly edge-on. The system is detached. However, we cannot rule out lower inclinations

that would give larger values of the mass and radius, implying some measure of evolution.

The eccentricity we determine is only marginally significant ($e = 0.0126 \pm 0.0049$, 2.6σ), and is possibly an artifact from distortions in the velocities related to surface activity, given the short orbital period (2.55 days) and convective envelopes of the stars. Alternate designation TYC 690-1116-1.

[30] RXJ0441.9+0537. This double-lined binary (also BD+05°706) is an Algol-type system (semi-detached) of a rare class referred to as “cool Algols”, of which only about a dozen examples are known. Both components are late-type giants, as opposed to one of them being an early-type dwarf, as in the “classical” Algols, and the system has undergone (and is perhaps still undergoing) mass transfer. Full details were reported by Torres, Neuhäuser & Wichmann (1998).

[31] RXJ0442.3+0118. SB2 system (TYC 83-788-1) with a circular orbit and a rather low mass ratio, indicating that one or both components are evolved. The light ratio is also quite small ($L_B/L_A = 0.16$). The cooler primary temperature (spectral type early K) suggests that this star must be the larger one, consistent with its larger mass. Its measured $v \sin i$ inserted into eq.(3) supports this, giving a $\log g$ value under 3.5, which we have adopted. The system is well detached. If the secondary is a main sequence star, a normal mass of $M_B \sim 0.81 M_\odot$ for its temperature suggests an inclination angle near 73° , although it could be larger. The minimum inclination angle for eclipses to occur, from eq.(3), is $i_{\min} \approx 77^\circ$. The possibility of eclipses cannot be ruled out, and photometric observations are underway to investigate this.

[32] RXJ0442.6+1018. The rotation of the primary in this long-period SB1 is small, but uncertain. Under the assumption that it is a main-sequence star (SpT \sim K2), the minimum mass for the secondary corresponds to a late-type M star. Tycho designation TYC 686-1246-1.

[33] RXJ0442.9+0400. Another object presenting triple-lined spectra. The velocities for the main component give a nearly circular orbit with a period of 510 days. The spectral type is approximately G7. The secondary component appears to be itself a double-lined binary, but the period is unknown. Weak Li I $\lambda 6708$ absorption was detected by M97, who suspected a possible PMS nature, while N97 considered it to be a ~ 100 Myr-old ZAMS system. The entry in the Tycho catalogue for this object (TYC 91-702-1) suggests photometric variability, as indicated by the scatter of ~ 0.9 mag in the V_T passband. Follow-up is warranted.

[34] RXJ0444.3+0941. The lines of the primary star in this single-lined system are very broad, consistent with the short period of the binary. The temperature we determine

corresponds approximately to spectral type F7. Synchronization and a typical radius for such a star ($1.22 R_{\odot}$) lead to an equatorial rotational velocity of 90 km s^{-1} . Our measured $v \sin i = 120 \text{ km s}^{-1}$ then implies an inclination angle near 49° . If the primary mass is normal ($1.27 M_{\odot}$), the secondary is of spectral type M3 or earlier, and is likely to be also a fast rotator. This system has also received the designation HD 287017.

[35] RXJ0444.4+0725. Short-period SB2 with a circular orbit. The components' rotation is most likely synchronized with the orbital motion. The secondary star is rather faint ($L_B/L_A = 0.13$) and its parameters correspondingly more uncertain. The mass ratio and light ratio are consistent with the standard mass-luminosity relation for dwarfs. Eq.(3) and the measured rotation of the primary also lead to a normal surface gravity for a main-sequence star. A typical mass for the primary of $M_A \sim 0.75 M_{\odot}$, based on its temperature, suggests an inclination angle of $i \sim 68^{\circ}$. However, the minimum angle for eclipses to occur in this system is $i_{\min} \approx 78^{\circ}$, so that eclipses seem to be ruled out. The system is well detached. Only weak Li I $\lambda 6708$ absorption was detected by M97, so that a PMS status for the object seems unlikely (see also §6.2).

[36] RXJ0451.6+0619. Single-lined binary with a circular orbit and a very short period. The temperature of the rapidly rotating primary corresponds to a spectral type of G8. Synchronization and a typical radius for a main-sequence star ($0.88 R_{\odot}$) gives an equatorial rotational velocity of about 64 km s^{-1} , whereas the value we measure is $v \sin i = 81 \text{ km s}^{-1}$. The star may be slightly evolved (larger). There is no clear sign of the secondary star in our spectra, despite the large value we infer for its minimum mass ($M_B \sin i \approx 0.76 M_{\odot}$), assuming a normal mass for the primary. A faint companion approximately $1''$ in the ENE direction was seen at the telescope.

[37] RXJ0503.6+1259. The secondary in this SB2 is extremely faint ($L_B/L_A = 0.07$), and its temperature and rotational velocity are very uncertain. From the very small mass ratio at least one of the stars must be evolved. Despite the short period the orbit appears to be slightly eccentric, although further observations are needed to confirm this. If real, the spins of the stars are likely to be synchronized with the orbital motion at periastron. In that case the measured $v \sin i$ of the primary translates into a size that is very close to that of the critical Roche surface for that star. Because the minimum masses are so small, the inclination angle is also likely to be small (10° to 30° for any reasonable values for the absolute masses). Therefore, the contribution of the last term in eq.(3) is not negligible (≈ 0.5 dex). Accounting for this, we have adopted $\log g_A = 3.0$. The nature of the secondary is unknown. The system appears to be similar to the Algols, or is possibly a W UMa-type object.

[38] RXJ0515.3+1221. This object (also known as TYC 707-1311-1) has a complicated

spectrum that appears to be triple-lined. The primary velocities yield an orbit with a period of 63 days. The secondary in this system is itself a binary, apparently double-lined. Although it has not been possible to determine its orbit, the period must be short since the velocity amplitudes of the secondary and tertiary components are at least 70 km s^{-1} . This is likely to be the source of the X-ray radiation detected by ROSAT. There is a faint visual companion approximately $20''$ the south of this triple system.

[39] **RXJ0523.0+0934.** The short period and circular orbit make synchronization very likely in this SB1 system. The measured $v \sin i$ is in good agreement with the value predicted assuming a normal radius of $1.25 R_{\odot}$ for a main-sequence star of the temperature we measure (which corresponds to F6 V, and $1.3 M_{\odot}$). This, in turn, implies an orbit viewed nearly edge-on. The minimum mass for the secondary corresponds roughly to an M3 star. The object (TYC 704-975-1) is listed in the Tycho catalogue as having a scatter of 0.4 mag in the V_T passband, although this needs confirmation. The system is most likely detached.

[40] **RXJ0523.5+1005.** The rapid rotation of the components in this SB2 system is due to the very short orbital period (0.55 days). However, the predicted equatorial rate assuming synchronization is nearly twice the measured $v \sin i$ values, implying a fairly low inclination angle. Adopting masses for main-sequence stars ($0.9 M_{\odot}$ and $0.8 M_{\odot}$) consistent with the measured temperatures, we derive $i \sim 27^{\circ}$, although this inclination together with our measured $v \sin i$ values gives radii slightly larger than normal for stars of this spectral type (G7 and K0): $1.2 R_{\odot}$ and $0.9 R_{\odot}$. Eclipses are not expected for inclinations lower than $i_{\min} \approx 50^{\circ}$. The system is probably still detached, although the primary star appears to be rather close to filling its Roche lobe (90%). The light ratio is $L_B/L_A = 0.22$. Tycho designation TYC 704-2521-1.

[41] **RXJ0528.9+1046.** The assumption of synchronization in this 7.7-day period double-lined binary along with our measured values of $v \sin i$ implies low surface gravities for both components. From eq.(3) we derive $\log g = 3.5$, ignoring the contribution from the term that depends on the unknown inclination. The system is well detached, and the light ratio at 5187 \AA is $L_B/L_A = 0.34$. The lower limit for eclipses to occur is $i_{\min} \approx 77^{\circ}$, but the small minimum masses suggest that the actual inclination is considerably lower than this. Our formal spectroscopic solution gives an orbit with a small but apparently significant eccentricity: $e = 0.0290 \pm 0.0071$ (4σ). This is somewhat unexpected for the relatively short period and the fairly deep convective envelopes of the late-type components, and could be caused by distortions in the measured radial velocities due to chromospheric activity (spots). Even if the eccentricity is real, the spins of the stars are likely to be synchronized with the orbital motion at periastron, and the values inferred above for the surface gravity

still hold.

From the dynamical evidence the stars are larger than normal dwarfs. One possibility is that they are both subgiants or giants of spectral type early- or mid-K, quite typical of the RS CVn class. However, the presence of very strong Li I $\lambda 6708$ absorption and other clues suggest otherwise. The object is projected against the λ Ori star-forming region, and its center-of-mass velocity of $+28.3 \pm 0.2 \text{ km s}^{-1}$ is consistent with the mean velocity of other objects in that complex. M97 measured a Li absorption strength of 0.4 \AA , at an epoch when the spectral lines of the two components were severely blended. More recently Dolan & Mathieu (2001) established that both stars show very prominent Li lines. After correction for binarity using an estimated light ratio of $L_B/L_A = 0.5$ at $\lambda 6708$, their raw measurements correspond to equivalent widths 0.40 \AA and 0.45 \AA for the primary and secondary, respectively. The Li excess over the levels displayed by stars of similar temperatures in young clusters such as the Pleiades or IC 2602 is strongly indicative of a very young age (see N97), and supports its classification as a wTTS (see also Magazzù et al. 1999). *VRI* photometry by Dolan & Mathieu (2001), along with an assumed distance of 450 pc for the λ Ori region, led them to an estimated age of 2.3 Myr for RXJ0528.9+1046, using the stellar evolution models by Palla & Stahler (1999). The conclusion of the PMS nature for this object is further supported by our independent comparison with evolutionary tracks in §6.2.

[42] **RXJ0529.3+1210.** The orbit in this long-period binary is extremely eccentric ($e \geq 0.9$), and because of this the elements are still preliminary. The appearance of the correlation functions and the large minimum secondary mass we derive from our single-lined orbit suggest there may be light from another star, or possibly from two additional stars. The temperature of the primary corresponds roughly to a spectral type of K6, if it is a dwarf. The $v \sin i$ value we measure (18 km s^{-1}), however, is higher than expected for a normal main-sequence star. It is possible that the axial rotation is synchronized with the orbital motion at periastron (“pseudo-synchronized”), which, by virtue of the exceptionally large eccentricity, would be considerably faster than the mean orbital motion by a factor of more than 50. If that is the case, the projected radius of the star would be $R \sin i = 2.9 R_{\odot}$. This is much larger than normal for a K6 dwarf, suggesting in principle either a post-main sequence or a pre-main sequence status.

As in the previous system, RXJ0529.3+1210 is projected against the λ Ori complex, in this case towards the edge and coinciding with a density enhancement in the CO maps for this region (see Dolan & Mathieu 2001). The center-of-mass velocity of $+18.7 \pm 0.7 \text{ km s}^{-1}$, however, is more consistent with the mean for the Taurus-Auriga region, as noticed also for other stars in this area by Dolan & Mathieu (2001). This circumstantial evidence favors

the interpretation that this is a young system, rather than a highly evolved (post-main sequence) object. The Lithium strength as measured by M97 is 0.35 \AA , while we measure a slightly lower value of 0.27 \AA . Given the cool temperature of the primary, this further supports the notion that it is a relatively young system since cooler objects tend to deplete their primordial Lithium quite rapidly because of their deeper convective envelopes (see §6.1), and would not be expected to show such high levels. The $\text{H}\alpha$ emission is among the strongest in our sample. Both M97 and N97 considered it to be a PMS object. Magazzù et al. (1999) listed it as a post-T Tauri star.

[43] **RXJ0530.9+1227**. SB1 with a short period and a circular orbit. If the rotation of the primary is locked with the orbital motion, as expected, the lower limit to the radius based on eq.(2) and our measured $v \sin i$ is $R_A \sin i = 1.8 R_\odot$. This is about a factor of 2 larger than normal for a main sequence star with the temperature we determine, which indicates that the star is probably evolved (spectral type late G). Accordingly, we have adopted a lower surface gravity of $\log g = 4.0$. The residuals from the orbit show a pattern suggestive of a long-term variation ($P > 5 \text{ yr}$). The center-of-mass velocity of this system, $+92.4 \text{ km s}^{-1}$, is the largest in our sample.

6. Discussion

6.1. Lithium strengths and PMS status

The original selection of the N97 sample, while designed to favor the detection of young stars in a flux-limited X-ray survey (RASS), has obviously not been completely successful as attested by the large fraction of (post-main sequence) RS CVn systems among our binaries. Nevertheless, a handful of our program stars do have detectable Li I $\lambda 6708$ absorption, one of the key diagnostics of youth used to support PMS status. Because the strength of the Lithium line depends quite strongly on the effective temperature, and even on the rotational velocity of the star (see, e.g., Soderblom et al. 1993; Martín & Claret 1996), both of these parameters must be accounted for to evaluate the significance of the Li signature. Even with this, additional information on the systems can also be very helpful, such as that provided by our orbital solutions in §4 and §5.

In Figure 5 we represent the Li measurements as a function of effective temperature for the 10 objects in our sample with equivalent widths larger than 0.1 \AA , as listed in Table 1. For stars with more than one measurement we have adopted the average. Six systems are double-lined, but only two have separate measurements for the two components. For the others, we have adopted the temperature of the brighter component and assumed that the

Li measurement corresponds largely to that star. The measurements for all double-lined systems have been corrected for the dilution factor due to binarity, using our temperature determinations and approximate light ratios at 6708 Å estimated from our measurements at 5187 Å.

The segmented lines in the Figure 5 represent the upper envelope of the Li distributions for two young clusters often used for comparison purposes — IC 2602 (age ~ 35 Myr), and the Pleiades (age ~ 100 Myr) — following N97. For the latter cluster, which has been studied in considerably more detail, the rapid rotators ($v \sin i > 15 \text{ km s}^{-1}$) display somewhat lower Li depletion (larger equivalent widths) than the slow rotators, as represented by the solid and long-dashed lines, respectively.

Three of our systems deserve special comment. The cooler component of [24] RXJ0422.9+0141 lies slightly above the upper envelope for IC 2602, suggesting the possibility of a PMS status. However, the dynamical and physical information discussed in §5 seems to rule this out (see also below), since the larger mass for this cooler component indicates that this star must have evolved to become a subgiant or a giant. We conclude therefore that this is a post-main sequence system of the RS CVn type. Studies by Pallavicini, Randich & Giampapa (1992), Fernández-Figueroa et al. (1993), Randich, Giampapa & Pallavicini (1994) and others have shown that active systems of the RS CVn type and other categories of active objects occasionally show unexpectedly high levels of Li absorption compared to inactive stars of similar spectral types. While the mechanism responsible for the excess Li abundance is not yet clear, the case of [24] RXJ0422.9+0141 appears consistent with those findings.

The two components of [41] RXJ0528.9+1046 show significant excess Li absorption, and the supplementary evidence discussed in §5 strongly supports its classification as a weak-lined T Tauri system. The Li strength measured for [42] RXJ0529.3+1210 puts it essentially at the upper envelope of IC 2602, but this may be only a lower limit since there are hints in our spectra of light from one or perhaps two additional components. This extra light would cause the true equivalent width of the primary to be underestimated, though it is difficult at the moment to determine by how much. Based on this and the strong suggestion of association with the λ Ori region discussed in §5, we consider it quite likely that this system is also very young.

Thus, two of our program stars display properties indicating that they are PMS objects with ages most likely under ~ 30 Myr. The fact that they are binaries makes them especially interesting, given that only about three dozen such objects have had their spectroscopic orbital elements determined. Furthermore, [42] RXJ0529.3+1210 is among only a handful with periods long enough that the components may be spatially resolved in the near future

using large ground-based interferometers observing in the infrared. At these wavelengths the contrast between the primary and secondary components should be much more favorable than in the optical. At an assumed distance of 450 pc for [42] RXJ0529.3+1210 (Dolan & Mathieu 2001) the angular semimajor axis of the pair is estimated to be about 3 mas. But because of the large eccentricity of its orbit, the maximum separation can be as large as twice this value.

6.2. A comparison with evolutionary tracks

In §5 we made use of the measured $v \sin i$ values for the short-period double-lined binaries in our sample that have circular orbits, in order to provide estimates of the radii and surface gravities of the components and help in understanding their nature. In a sense the rotational velocities have thus been used as a sensitive measure of evolution, under the reasonable hypothesis that tidal forces have already synchronized the rotation of the stars and aligned their axes with that of the orbit. Those estimates are only lower limits, though, because of the unknown inclination angles. In this section we take this approach one step further and eliminate the dependence on i to provide a physical magnitude that may be compared directly with predictions from theory for normal stars.

Eq.(1) and eq.(2) give the quantities $M \sin^3 i$ and $R \sin i$ directly in terms of observable properties (P , K , and $v \sin i$). The minimum masses and minimum radii have different dependences on $\sin i$, but the ratio $M \sin^3 i / (R \sin i)^3$ removes the dependency, and happens to represent the *density* of a star (M/R^3) in terms of the solar density. Expressed directly as a function of the measurable parameters, we have

$$\log \frac{\rho_{A,B}}{\rho_{\odot}} = -1.8718 - 2 \log P + 2 \log(K_A + K_B) + \log K_{B,A} - 3 \log V_{A,B}^{\text{rot}} , \quad (6)$$

where all quantities are given in their usual units. The density is intimately related to the internal structure and evolutionary status of a star, and the possibility of using this “observable” property in suitable double-lined systems to compare directly with stellar evolution models is often overlooked⁶. The density changes by more than two orders of magnitude over the life of a normal star, so that at the very least this allows us (in conjunction with the measured effective temperatures) to tell whether the components are still on the main sequence or whether they are evolved. As it turns out, the discriminating power of the density is quite significant although it depends greatly on the precision of the rotational velocities, as seen from the factor of 3 in the last term of eq.(6).

⁶For a recent application of this idea, see Quast et al. (2000).

In Figure 6 we show the components of all the double-lined systems in our sample that have sufficiently well determined rotational velocities, in a diagram of $\log \rho/\rho_{\odot}$ vs. $\log T_{\text{eff}}$. In all cases the periods are short or there is otherwise good reason to believe that the assumption of synchronization and alignment is valid, as described in the individual notes for each system. In each binary a dotted line connects the primary components (dark symbols) with the secondaries (open symbols, with the identification number). The observations are compared with theoretical isochrones for the main-sequence and post-main-sequence phase based on the models by Yi et al. (2001), for solar metallicity and ages of 1 Gyr, 3 Gyr, 10 Gyr and 15 Gyr.

Almost all of the secondary components are seen to lie near the main sequence, while roughly half of the primaries are evolved and lie at the base of the giant branch or above. A gap is seen in the diagram between the evolved and un-evolved stars that coincides with the locus of objects in the rapid subgiant phase, where fewer stars are expected at any given time. For the most part the two components of each binary are consistent with being on a single isochrone, given the errors, the most obvious exceptions being [12] RXJ0309.1+0324N and [41] RXJ0528.9+1046, which seem to be aligned in a direction roughly perpendicular to the isochrones. The first of these is most likely a W UMa-type system, and its components should therefore not be expected to behave as single stars since they are in close mechanical and thermal contact. The evidence presented earlier for the other system indicates that it is likely to be in the PMS stage (see below). But for all the other objects, we note that the location of each star is fully consistent with our interpretation in §5. This is expected since the same hypothesis was used, but the evolutionary status of each binary is more straightforward to see and to compare with the models in this figure.

The densities of the primary components in all the binaries are typically smaller than those of the secondaries, as dictated by stellar evolution, except in the case of [30] RXJ0441.9+0537, which is the highest object on the diagram in Figure 6. In this system (which is the “cool Algol” referred to earlier) mass transfer has caused a reversal of the mass ratio, so that the currently more massive star is actually the one that was originally the secondary (see Torres, Neuhäuser & Wichmann 1998).

As mentioned earlier, a few of our systems exhibit moderately strong Li I $\lambda 6708$ absorption that may indicate an early stage of evolution (PMS), as opposed to a post-main sequence status. Six of them are double lined. It is quite illuminating to represent these systems in a $\log \rho/\rho_{\odot}$ vs. $\log T_{\text{eff}}$ diagram such as Figure 6, but to compare them instead with evolutionary tracks appropriate for the PMS stage. This is done in Figure 7, where the isochrones and evolutionary tracks are from the models by Siess, Forestini & Dougados (1997) (see also Siess, Dufour & Forestini 2000) for solar metallicity.

The components of [5] RXJ0219.7–1026, [14] RXJ0339.6+0624, [16] RXJ0343.6+1039, and [24] RXJ0422.9+0141 are clearly inconsistent with being on the same isochrone, and this agrees with our assessment in §5 that they are not likely to be in the PMS phase based on dynamical and physical evidence (e.g., the mass ratio and luminosity ratio), or based on their relatively weak Li line in most cases (§6.1). Objects [35] RXJ0444.4+0725 and [41] RXJ0528.9+1046, on the other hand, do seem to conform to the isochrones in this diagram, within the errors. The age inferred for the first of these is not particularly young, and its properties (including the weak Li absorption) are consistent with it being a ZAMS star. The location in the $\log \rho/\rho_{\odot}$ vs. $\log T_{\text{eff}}$ plane is also consistent with the main-sequence isochrones shown in Figure 6, so that the case for a PMS status is not very strong in this system.

More interesting is the agreement of [41] RXJ0528.9+1046 with the PMS isochrones in Figure 7, while running *across* those in Figure 6. This, along with the Li strengths and kinematic information reported earlier, makes a more compelling case for this system being a much younger object. The absence of H α emission reported by M97 and by Dolan & Mathieu (2001) place it in the wTTS category. The age we derive for this SB2 from Figure 7 is approximately 2 Myr, consistent with the estimate of 2.3 Myr by Dolan & Mathieu (2001) based on a different set of models (Palla & Stahler 1999). Use of yet another set of PMS isochrones by Yi et al. (2001) yields a younger age of about 1 Myr. The absolute masses for the components from this figure ($M_A = 1.96 M_{\odot}$ and $M_B = 1.46 M_{\odot}$) are not quite consistent with the spectroscopic mass ratio, which is measured much more accurately. This is most likely due to errors in the temperature determinations. In addition, the absolute masses are strongly model-dependent. For example, the values inferred from the PMS evolutionary tracks by Yi et al. (2001) are systematically lower by 0.4–0.5 M_{\odot} , which is rather significant. Nevertheless, one may derive an average inclination angle for the orbit that is roughly 33–37°, which rules out eclipses, as indicated in §5.

It is worth pointing out, to conclude this section, that a diagram such as Figure 7 can be a very useful tool in the field of young stars, specifically for the case of double-lined spectroscopic binaries with short periods and circular orbits. It is similar to the more widely used H-R diagram, but has the important advantage that it is completely independent of any assumption on the distance, a common criticism that is painfully familiar to all users of the $\log L/L_{\odot}$ vs. $\log T_{\text{eff}}$ diagram.

6.3. Period distribution and binary frequency

In the course of solving for the orbits of the binaries in the N97 sample we had the distinct impression that the fraction of short-period systems was unusually high. Due to the nature of the target list, which was selected to include objects that are strong in X-rays, a bias towards short periods is actually expected from the fact that those systems will tend to be rotating faster because they are tidally locked, and thus will have enhanced activity and should be detected more easily by ROSAT. As it turns out, more than half of our binaries have orbital periods of less than 5 days. In addition, we noticed two other trends that were not expected for field stars, but in retrospect can also be understood in terms of selection effects. One is that the frequency of binaries among the ROSAT sources south of Taurus seemed higher than normal (43 spectroscopic binaries with orbits, out of a sample of 121 stars), and the other is that the fraction of double-lined systems (as opposed to single-lined binaries) also seemed high: 26 SB2 systems out of 43 binaries, or 60%.

The detection of spectroscopic binaries in our sample is by no means complete as a function of orbital period. The majority of the stars were observed over an interval of 3 to 5 years, and we estimate conservatively that we have detected most of the systems with orbital periods up to about 1 yr, although we also found 3 binaries with even longer periods. The incompleteness due to small velocity amplitudes (low-mass companions, small inclinations, or both) is difficult to quantify, but it is unlikely to be very large for this sample and will not be considered here.

As a benchmark for studying the frequency and period distribution of the binaries in our X-ray sample we have used the results for the solar-type stars in the solar neighborhood by Duquennoy & Mayor (1991). In Figure 8 we show the period distribution for the 43 binaries in our sample compared to the corresponding distribution for the field, on a logarithmic scale. The normalization was computed by requiring that the integral of the smooth curve up to periods of 1 yr (our completeness level, represented with a dashed line) is equal to the number of binaries detected in our sample up to that period (40). The hatched area of the histogram represents the double-lined systems, and the open area added above is for the SB1 binaries.

The observed distribution of X-ray binaries is sharply peaked at short periods (median $\log P = 0.67$, or a period of 4.7 days) and shows an excess over the field distribution, as anticipated above. The frequency of binaries in our sample (40 systems detected up to our completeness limit of 1 yr, out of 121 objects studied) is $33\% \pm 5\%$. This is nearly double the fraction of binaries in the field up to this period, which is $17\% \pm 3\%$. If we choose a more conservative completeness limit for our sample of, say, 100 days, the excess of binaries would be even greater since the number of systems detected in our sample up to 100 days

remains the same, yet the binary frequency in the field decreases to $11\% \pm 2\%$.

The increased fraction of binaries compared to the field is understood as a selection effect, since binaries will tend to be brighter than single stars in X-rays, not only because they are composed of two objects, but also because of the increased activity if the period is short. They will thus tend to be promoted into the (flux-limited) sample more easily compared to single stars. A similar effect can explain why SB2 systems dominate over SB1 systems.

6.4. Activity

Correlations between some of the physical properties of the stars and a number of activity indicators might in principle be expected to exist in a sample such as ours, composed largely of RS CVn-type or similarly active systems. For example, we searched for a dependence of the X-ray hardness ratios HR1 and HR2 and also the X-ray flux of our binaries (using data as reported by M97) with parameters such as the orbital period, the effective temperature, the projected rotational velocity, and the surface gravity. No significant correlations were found, possibly because essentially all of our objects are active by virtue of their selection. For the double-lined systems where there is ambiguity as to which component's parameters to use, we considered alternatively those of the coolest component, the more massive component, and also the visually brightest component, with null results in all cases. No differences were found between the X-ray properties of the single-lined binaries and the double-lined binaries, with the possible exception of a hint that the SB2 systems may have systematically larger HR2 indices (by about 0.10-0.20), indicative of slightly harder X-ray emission.

Similarly, examination of correlations between the $H\alpha$ emission as given by M97 (equivalent width) and the orbital or stellar characteristics $\log P$, $v \sin i$, or $\log g$ indicated no dependence. There is, however, a clear dependence with effective temperature, in the sense that cooler systems tend to have stronger $H\alpha$ emission. This is consistent with the fact that stars with lower temperatures are typically more chromospherically active. The correlation is shown in Figure 9a for the single-lined systems in our sample (triangles). Negative equivalent widths indicate emission, while positive values represent absorption (which may be partially filled-in in some cases). Although there appears to be a similar correlation for the double-lined systems (not shown), the scatter is much larger because of the confusion as to which component the emission measured by M97 corresponds to.

It is of interest to compare the trend for the single-lined binaries with that for the

single stars in the N97 sample, which we have represented by crosses in Figure 9a. The temperatures for these single stars were derived using the same technique we have applied in this paper. The increase in H α equivalent width for the cooler objects is again obvious. The slope of the correlation is essentially the same in both cases, but the binaries appear to lie slightly higher on the diagram. To test the statistical significance of this we carried out a linear fit to all the data (SB1 + singles) and examined the residuals from this fit separately for the SB1 systems and the single stars. The slope of this correlation is $d(\text{H}\alpha)/dT_{\text{eff}} = +0.236 \pm 0.026 \text{ \AA per 100 K}$. Figure 9b shows the distributions of residuals. The SB1 systems have equivalent widths that are $0.56 \pm 0.18 \text{ \AA}$ more negative, on average, indicating stronger emission (a 3.1σ effect).

To examine whether this excess emission compared to the single stars might be due to a difference in rotational velocities, we show in Figure 10a the $v \sin i$ distributions for the single stars and for the SB1s. Despite expectations (tidal locking in close binaries), the distributions are not statistically different, as indicated by the Kolmogorov-Smirnov test. As it turns out, a significant fraction of the binaries have long orbital periods, and are therefore not yet affected by tidal effects. The reason for the slightly stronger H α emission for the binaries in our sample is thus not obvious.

The vertical scatter in Figure 9a, particularly for the single stars, does appear to be related to the rotation of the stars. In Figure 10b we show the residuals from the H α vs. T_{eff} correlation as a function of the rotational velocity of the objects, separately for the single stars and the binaries. The residuals for both types of objects have been corrected for the systematic difference found above. The trend for the single stars goes in the direction expected, namely, the fast rotators show extra emission and the slow rotators show less. There appears to be no such trend for the single-lined binaries, although the sample is small.

7. Final remarks

High-resolution spectroscopic monitoring of ROSAT X-ray sources south of the Taurus-Auriga star-forming region has resulted in the discovery of numerous binary systems in the N97 sample. In this paper we report new spectroscopic orbital solutions for 42 systems, along with determinations of the physical characteristics (effective temperature, projected rotational velocity, surface gravity, estimated masses and radii) of all visible components. Detailed descriptions of each system have been provided to facilitate follow-up in particularly interesting cases.

The original selection of the N97 sample was designed to increase the likelihood of including young stars associated with the star-forming region, but at least in the case of the binaries that we have turned up, it has generally yielded field objects of a rather different nature than intended, ranging from contact systems of the W UMa type and mass-exchange Algols to active main sequence binaries. The overall properties of these systems (strong excess of short-period binaries, large fraction of double-lined systems) as well as the high frequency of binaries compared to the number of original targets in the sample can all be understood in terms of the selection criteria, since these properties all tend to make the objects brighter in X-rays. The finding that a significant fraction of the ROSAT X-ray sources are active binaries is consistent with results in other regions of the sky, including old open clusters such as M67 (see, e.g., Belloni, Verbunt, & Schmitt 1993; Belloni, Verbunt, & Mathieu 1998; van den Berg, Verbunt, & Mathieu 1999), even though the biases may be somewhat different. It seems likely, therefore, that surveys of ROSAT X-ray sources in other areas of the sky using similar criteria to promote the detection of PMS stars will also result in a possibly substantial fraction of the objects being active binary systems instead. However, that fraction could depend strongly on the region or on the distance from the molecular gas.

While most of our binary systems fall into the RS CVn category, the selection has at least been successful in two cases where other evidence (Li I λ 6708 absorption, kinematics, proximity to other young objects, dynamical evidence based on our orbital solutions) shows quite convincingly that the objects are truly young. [41] RXJ0528.9+1046 is a double-lined binary with a period of 7.7 days that is most likely associated with the λ Ori region, and may be as young as 2 Myr. [42] RXJ0529.3+1210 is a very eccentric single-lined binary with an orbital period of 463 days, also a probable member of the same region. Both are classified as wTTS based on their weak H α emission. These systems add to the still relatively small population of PMS binaries with known orbital elements, the study of which may hold important clues to the process of binary star formation.

Among other interesting systems we have discovered is a potentially important eclipsing binary, [6] RXJ0239.1–1028, composed of a pair of detached K stars. Such objects are relatively rare, and are particularly valuable to test models of stellar evolution in the lower main sequence. Three other systems in our sample are also very likely to be eclipsing, and should be followed up: [3] RXJ0212.3–1330, [12] RXJ0309.1+0324N, and [31] RXJ0442.3+0118. The second of these is a W UMa-type binary.

Finally, the short-period systems in our sample with circular orbits have provided us with the opportunity to apply a simple but effective tool for the study of double-lined binaries in general, and young systems in particular, which is often overlooked: the use

of the stellar density as a sensitive measure of evolution. Under favorable conditions the density can be derived directly from the spectroscopic orbital elements and the measured projected rotational velocities, and can serve as a substitute for the luminosity in the familiar H-R diagram, with the advantage of being completely independent of distance. The experience gained from the systems studied here shows that it can be a useful diagnostic in some cases for distinguishing between main sequence and PMS status, and for comparing with stellar evolution models.

Many of the spectroscopic observations for this project were obtained at the CfA telescopes by P. Berlind, M. Calkins, J. Caruso, R. J. Davis, J. Degnan, D. W. Latham, A. A. E. Milone, J. Peters, R. P. Stefanik, and J. Zajac. We are grateful to R. J. Davis for also maintaining the CfA database of radial velocities, and to Sabine Frink, who provided proper motion information for some of our targets. A number of helpful comments by an anonymous referee are also acknowledged. This research has made use of the SIMBAD database, operated at CDS, Strasbourg, France, and of NASA's Astrophysics Data System Bibliographic Services.

REFERENCES

- Alcalá, J. M., Covino, E., Torres, G., Sterzik, M. F., Pfeiffer, M. J., & Neuhäuser, R. 2000, *A&A*, 353, 186
- Alcalá, J. M., Krautter, J., Schmitt, J. H. M. M., Covino, E., Wichmann, R. & Mundt, R. 1995, *A&AS*, 114, 109
- Alcalá, J. M., Terranegra, L., Wichmann, R., Chavarría, K. C., Krautter, J., Schmitt, J. H. M. M., Moreno-Corral, M. A., de Lara, E. & Wagner, R. M. 1996, *A&AS*, 119, 7
- Belloni, T., Verbunt, F., & Mathieu, R. D. 1998, *A&A*, 339, 431
- Belloni, T., Verbunt, F., & Schmitt, J. H. M. M. 1993, *A&A*, 269, 175
- Carney, B. W., Latham, D. W., Laird, J. B., & Aguilar, L. A. 1994, *AJ*, 107, 2290
- Covino, E., Alcalá, J. M., Allain, S., Bouvier, J., Terranegra, L., & Krautter, J. 1997, *A&A*, 328, 187
- Dolan, C. J., & Mathieu, R. D. 2001, *AJ*, 121, 2124
- Duquennoy, A., & Mayor, M. 1991, *A&A*, 248, 485
- ESA 1997, *The Hipparcos and Tycho Catalogues*, ESA SP-1200
- Fernández-Figueroa, M. J., Barrado, D., De Castro, E., & Cornide, M. 1993, *A&A*, 274, 373
- Gray, D. F. 1992, *The Observation and Analysis of Stellar Photospheres*, 2nd Ed. (Cambridge: Cambridge Univ. Press), 431
- Hut, P. 1981, *A&A*, 99, 126
- de Jager, C., & Nieuwenhuijzen, H. 1987, *A&A*, 177, 217
- Krautter, J., Wichmann, R., Schmitt, J. H. M. M., Alcalá, J. M., Neuhäuser R. & Terranegra, L. 1997, *A&AS*, 123, 329
- Kurtz, M. J., & Mink, D. J. 1998, *PASP*, 110, 934
- Latham, D. W. 1992, in *IAU Coll. 135, Complementary Approaches to Double and Multiple Star Research*, ASP Conf. Ser. 32, eds. H. A. McAlister & W. I. Hartkopf (San Francisco: ASP), p. 110
- Li, J. Z., & Hu, J. Y. 1998, *A&AS*, 132, 173
- Magazzù, A., Martín, E. L., Sterzik, M. F., Neuhäuser, R., Covino, E., & Alcalá, J. M. 1997, *A&AS*, 124, 449 (M97)
- Magazzù, A., Umana, G., & Martín, E. L. 1999, *A&A*, 346, 878
- Martín, E. L., & Claret, A. 1996, *A&A*, 306, 408

- Mathieu, R. D. 1994, *ARA&A*, 32, 465
- Melo, C. H. F., Covino, E., Alcalá, J. M., & Torres, G. 2001, *A&A*, 378, 898
- Murdoch, K. A., Hearnshaw, J. B., & Clark, M. 1993, *ApJ*, 413, 349
- Neuhäuser, R., Sterzik, M. F., Schmitt, J. H. M. M., Wichmann, R., & Krautter, J., 1995b, *A&A*, 297, 391
- Neuhäuser, R., Sterzik, M. F., Torres, G., & Martín, E. L. 1995a, *A&A*, 299, L13 (N95a)
- Neuhäuser, R., Torres, G. & Sterzik, M. F., & Randich, S. 1997, *A&A*, 325, 647 (N97)
- Neuhäuser, R., Walter, F. M., Covino, E., Alcalá, J. M., Wolk, S. J., Frink, S., Guillot, P., Sterzik, M. F., & Comerón, F. 2000, *A&AS*, 146, 323
- Nordström, B., Latham, D. W., Morse, J. A., Milone, A. A. E., Kurucz, R. L., Andersen, J., & Stefanik, R. P. 1994, *A&A*, 287, 338
- Palla, F., & Stahler, S. W. 1999, *ApJ*, 525, 772
- Pallavicini, R., Randich, S., & Giampapa, M. S. 1992, *A&A*, 253, 185
- Popper, D. M. 1992, in *IAU Symp. 151, Evolutionary Processes in Interacting Binary Stars*, ed. Y. Kondo, R. F. Sisteró & R. S. Polidan (Dordrecht: Kluwer), 395
- Press, W. H., Teukolsky, S. A., Vetterling, W. T., & Flannery, B. P. 1992, *Numerical Recipes*, 2nd. Ed. (Cambridge: Cambridge Univ. Press), 650
- Quast, G. R., Torres, C. A. O., de la Reza, R., da Silva, L., & Mayor, M. 2000, in *Birth and Evolution of Binary Stars*, *IAU Symp. 200*, eds. B. Reipurth & H. Zinnecker (Potsdam, Germany), p. 28
- Randich, S., Giampapa, M. S., & Pallavicini, R. 1994, *A&A*, 283, 893
- Schmidt-Kaler, Th. 1982, *Landolt-Börnstein: Numerical Data and Functional Relationships in Science and Technology*, eds. K. Schaifers & H. H. Voigt, (Springer-Verlag: Berlin), VI/2b
- Siess, L., Dufour, E., & Forestini, M. 2000, *A&A*, 358, 593
- Siess, L., Forestini, M., & Dougados, C. 1997, *A&A*, 324, 556
- Soderblom, D. R., Jones, B. F., Balachandran, S., Stauffer, J. R., Duncan, D. K., Fedele, S. B., & Hudon, J. D. 1993, *AJ*, 106, 1059
- Stefanik, R. P., Latham, D. W., & Torres, G. 1999, in *Precise Stellar Radial Velocities*, *IAU Coll. 170, ASP Conf. Ser.*, 185, eds. J. B. Hearnshaw & C. D. Scarfe (San Francisco: ASP), 354
- Sterzik, M. F., Alcalá, J. M., Neuhäuser, R., & Schmitt, J. H. M. M. 1995, *A&A*, 297, 418

- Torres, G., Neuhäuser, R., & Wichmann, R. 1998, *AJ*, 115, 2028
- van den Berg, M., Verbunt, F., & Mathieu, R. D. 1999, *A&A*, 347, 866
- Wichmann, R., Covino, E., Alcalá, J. M., Krautter, J., Allain, S., & Hauschildt, P. H. 1999, *MNRAS*, 307, 909
- Wichmann, R., Krautter, J., Schmitt, J. H. M. M., Neuhäuser, R., Alcalá, J. M., Zinnecker, H., Wagner, R. M., Mundt, R., & Sterzik, M. F. 1996, *A&A*, 312, 439
- Wichmann, R., Torres, G., Melo, C. H. F., Frink, S., Allain, S., Bouvier, J., Krautter, J., Covino, E., & Neuhäuser, R. 2000, *A&A*, 359, 181
- Yi, S., Demarque, P., Kim, Y.-C., Lee, Y.-W., Ree, C. H., Lejeune, T., & Barnes, S. 2001, *ApJ*, in press
- Zickgraf, F.-J., Alcalá, J. M., Krautter, J., Sterzik, M. F., Appenzeller, I., Motch, C., & Pakull, M. W. 1998, *A&A*, 339, 457
- Zucker, S., & Mazeh, T. 1994, *ApJ*, 420, 806
- Zucker, S., Torres, G., & Mazeh, T. 1995, *ApJ*, 452, 863

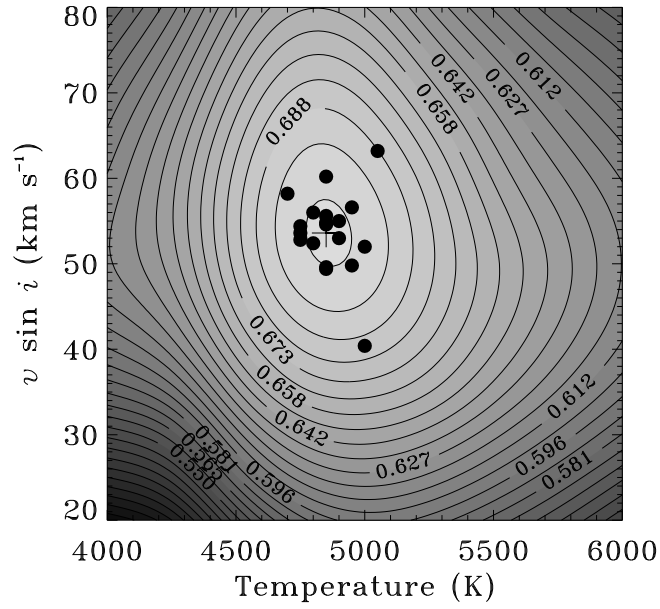


Fig. 1.— Determination of the effective temperature and rotational velocity of the single-lined binary [15] RXJ0340.3+1220. Contours represent the correlation value averaged over all exposures of the object, and the dots represent the parameters at the maximum correlation for each individual exposure. The peak of the average correlation is indicated by the plus sign ($T_{\text{eff}} = 4850$ K, $v \sin i = 54$ km s⁻¹).

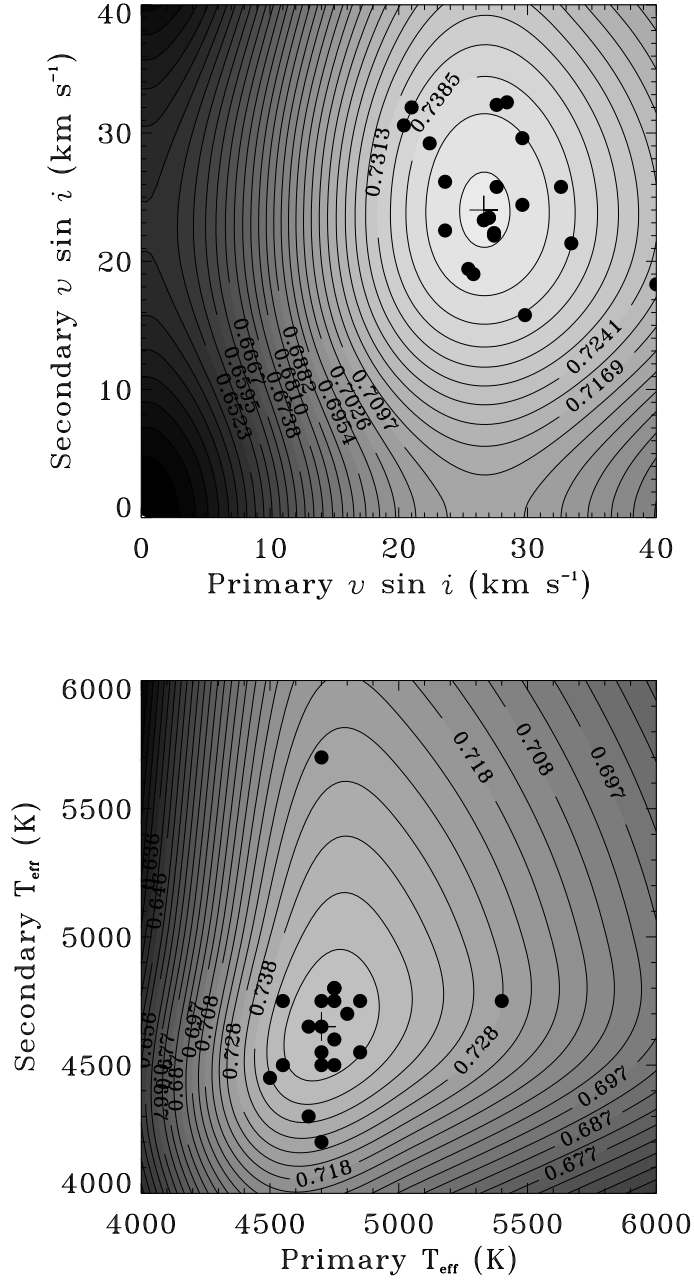


Fig. 2.— Same as Figure 1, but for the double-lined binary [8] RXJ0251.8–0203. The rotational velocities are determined first (top panel; $v_A \sin i = 27 \text{ km s}^{-1}$, $v_B \sin i = 24 \text{ km s}^{-1}$), and then fixed in order to determine the effective temperatures (bottom; $T_{\text{eff}}^A = 4700 \text{ K}$, $T_{\text{eff}}^B = 4650 \text{ K}$).

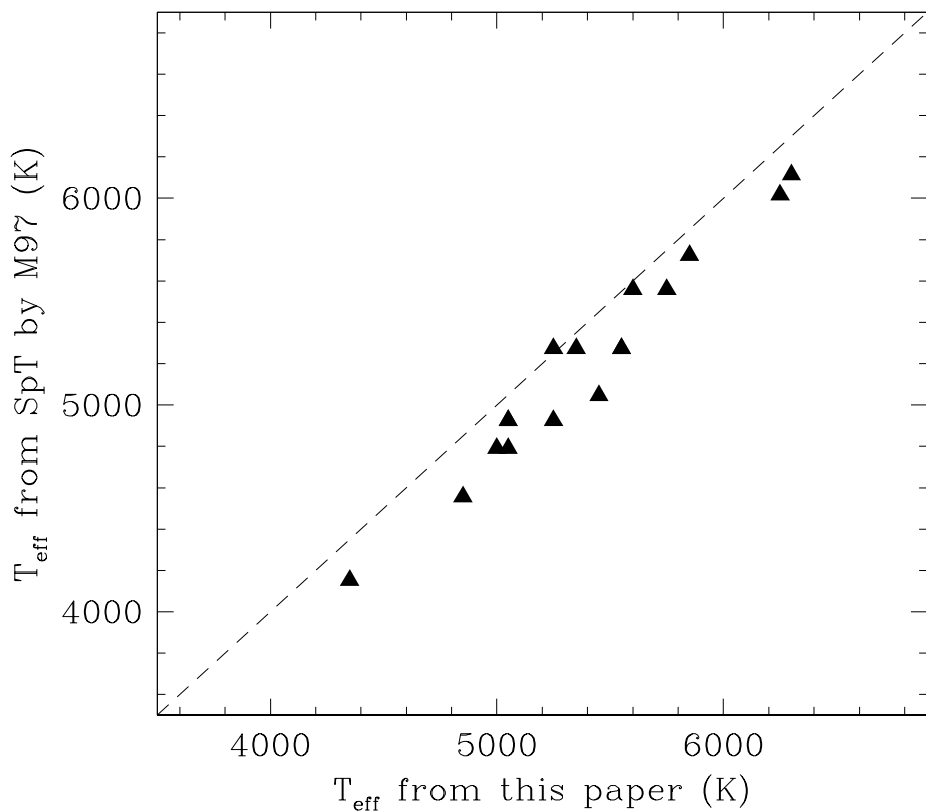


Fig. 3.— Comparison between the effective temperatures of the single-lined binaries in our sample derived from the M97 spectral types and the values determined here from fits to synthetic templates. Spectral types were converted to temperatures using the tabulation by Gray (1992). The offset of about 200 K from the diagonal line representing a perfect correlation is clearly seen.

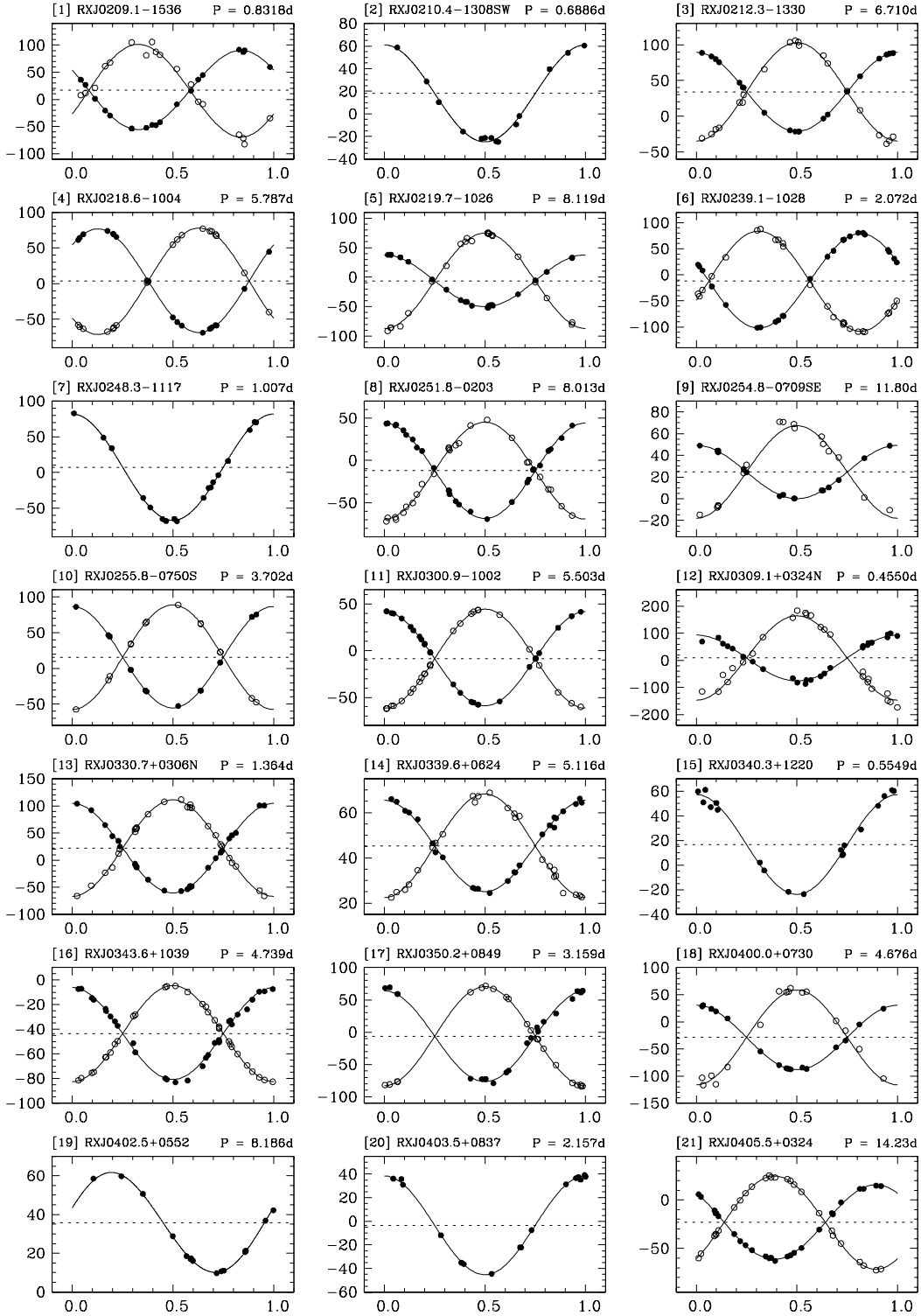
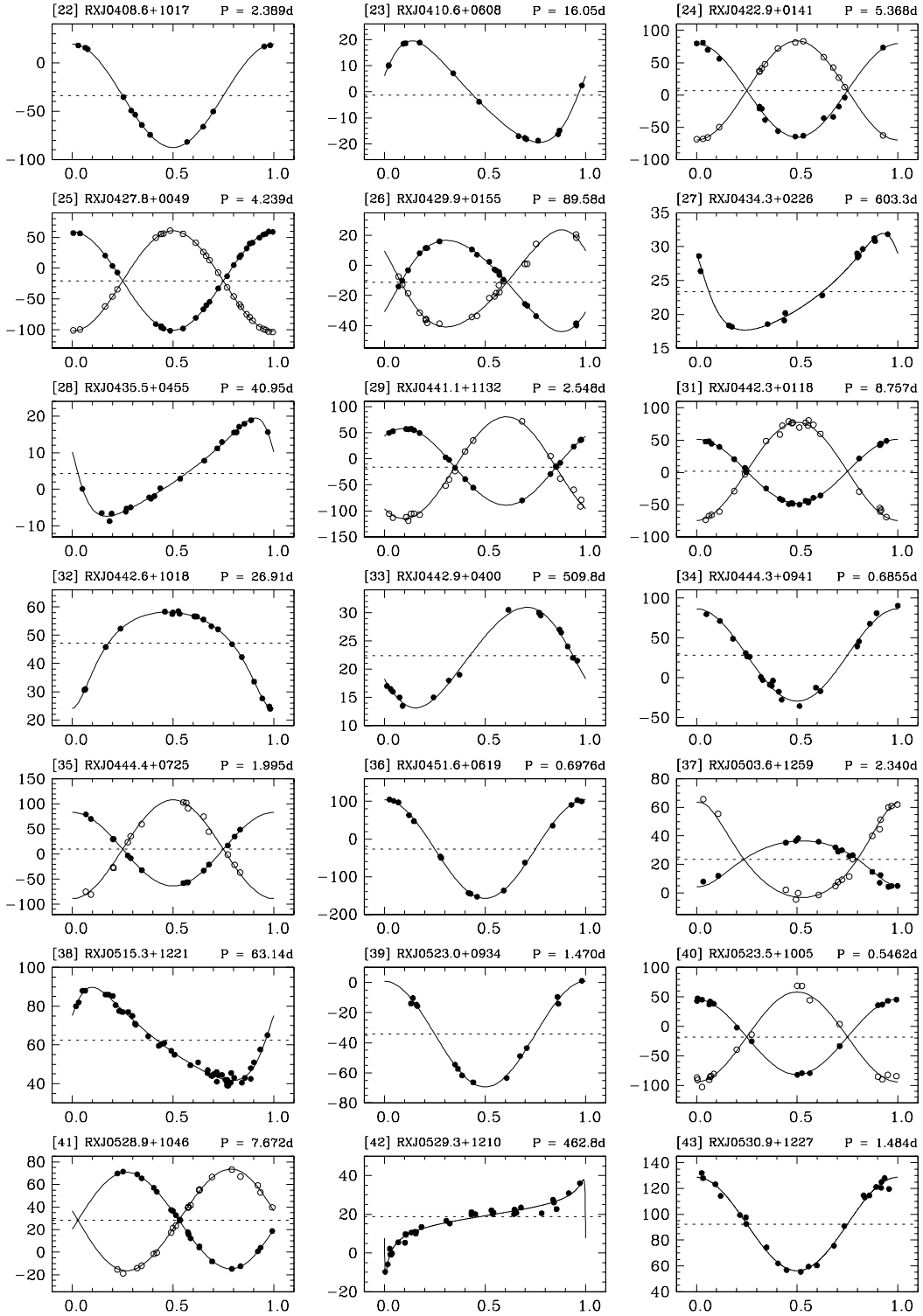


Fig. 4.— Orbital solutions for the single- and double-lined binaries, along with the observations. Each plot shows the radial velocity as a function of orbital phase. Filled symbols represent the primary velocities, and the dotted lines indicate the center-of-mass velocity of each system. (Continued on next page).



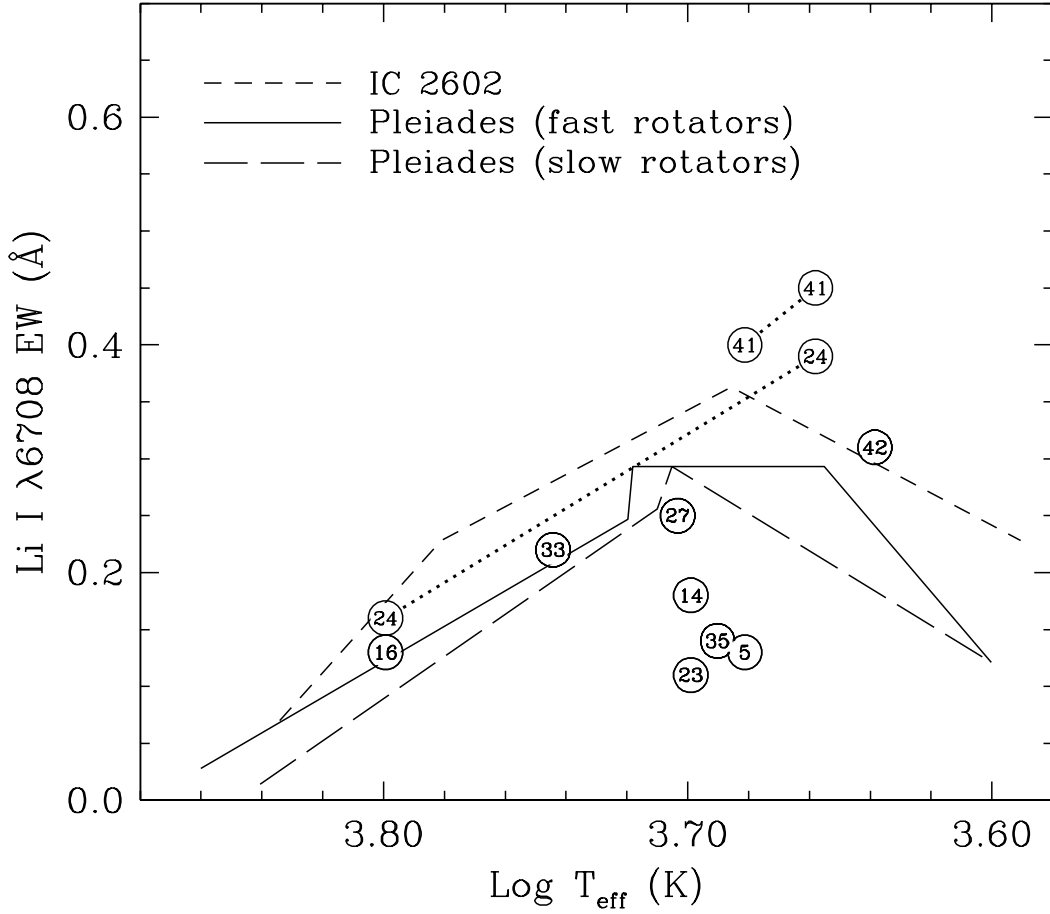


Fig. 5.— Li I $\lambda 6708$ equivalent widths from Table 1 for all systems in our sample with determinations exceeding 0.1 \AA (average values are taken when more than one measurement is available). The segmented lines represent the upper envelopes of the Li measurements as a function of temperature for the young cluster IC 2602 ($\sim 35 \text{ Myr}$) and for the Pleiades ($\sim 100 \text{ Myr}$) following N97. For the latter cluster separate envelopes are indicated for the rapid rotators and the slow rotators, with the dividing line set at $v \sin i = 15 \text{ km s}^{-1}$. The systems are identified by the running number in Table 1. Dotted lines connect the components of the double-lined binaries where separate measurements exist for the two stars.

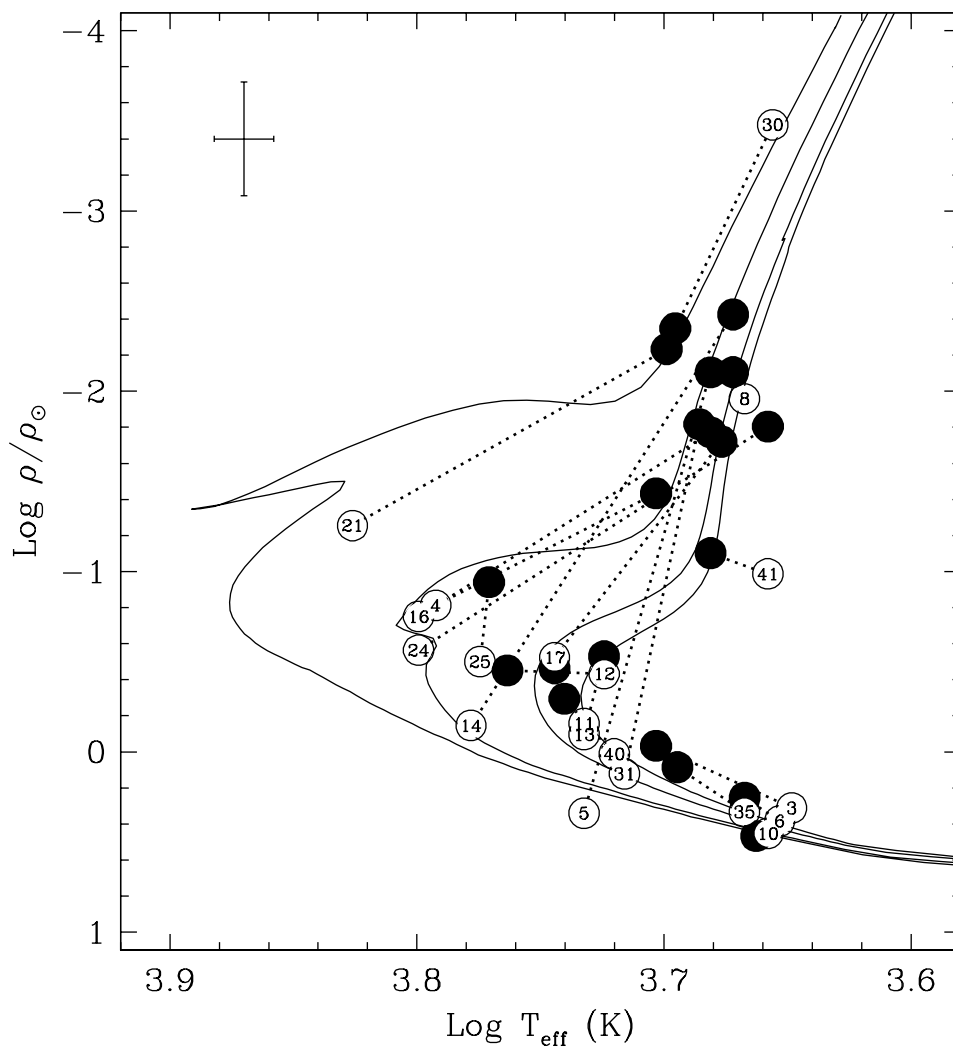


Fig. 6.— Double-lined binaries in the $\log \rho/\rho_{\odot}$ vs. $\log T_{\text{eff}}$ plane, compared to theoretical isochrones for the main sequence and post-main sequence phase by Yi et al. (2001) for solar metallicity and ages of 1 Gyr, 3 Gyr, 10 Gyr, and 15 Gyr (from left to right). The primary components (filled symbols) are connected to the secondaries (open symbols) by a dotted line. Systems are identified by the running number in Table 1. Average errors are indicated on the upper left, but vary significantly from system to system.

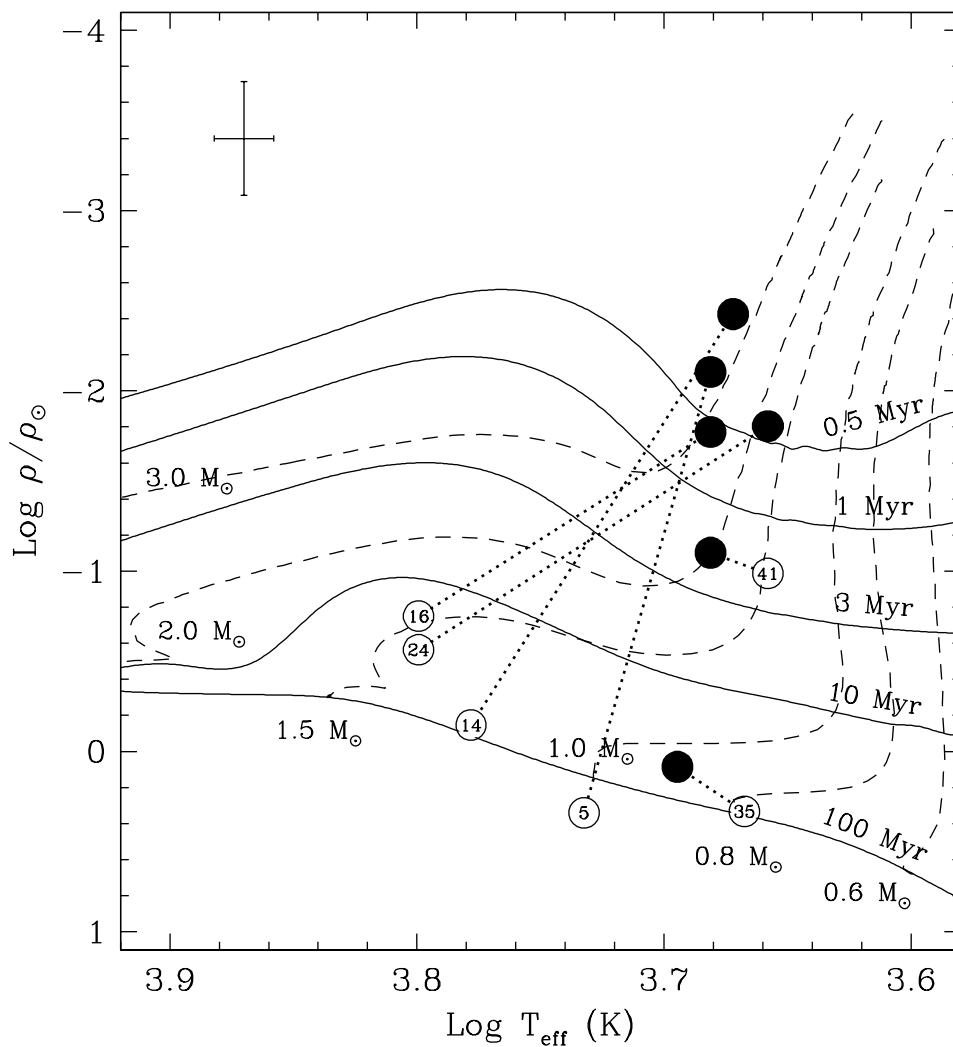


Fig. 7.— Same as Figure 6, but for PMS evolutionary tracks and isochrones from Siess, Forestini & Dougados (1997) for solar metallicity. Isochrones (solid curves) and mass tracks (dashed) are as labeled. All double-lined systems in our sample with measured Li I $\lambda 6708$ absorption larger than 0.1 \AA are represented for comparison (see text).

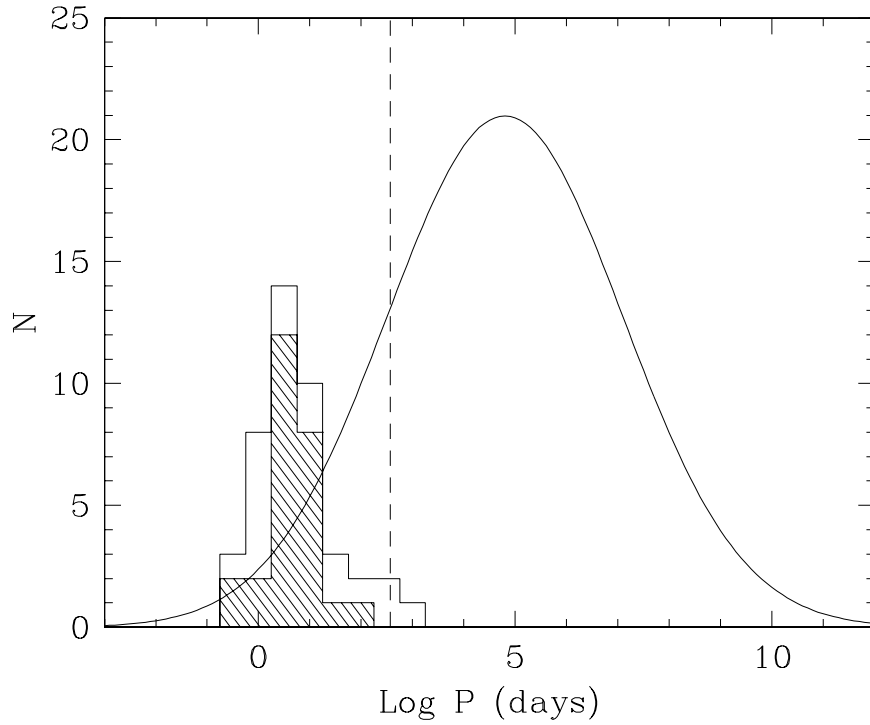


Fig. 8.— Period distribution (on a logarithmic scale) of the 43 binaries in the present sample compared to the solar-type binaries in the solar neighborhood. The hatched area of the histogram corresponds to the double-lined binaries in our sample, and the open area to the single-lined systems. The Gaussian curve representing the field binaries is taken from Duquennoy & Mayor (1991), and was normalized to yield the same number of systems that we detect up to our completeness level of 1 yr, indicated by the dashed line. The excess of short-period systems in the X-ray sample is discussed in the text.

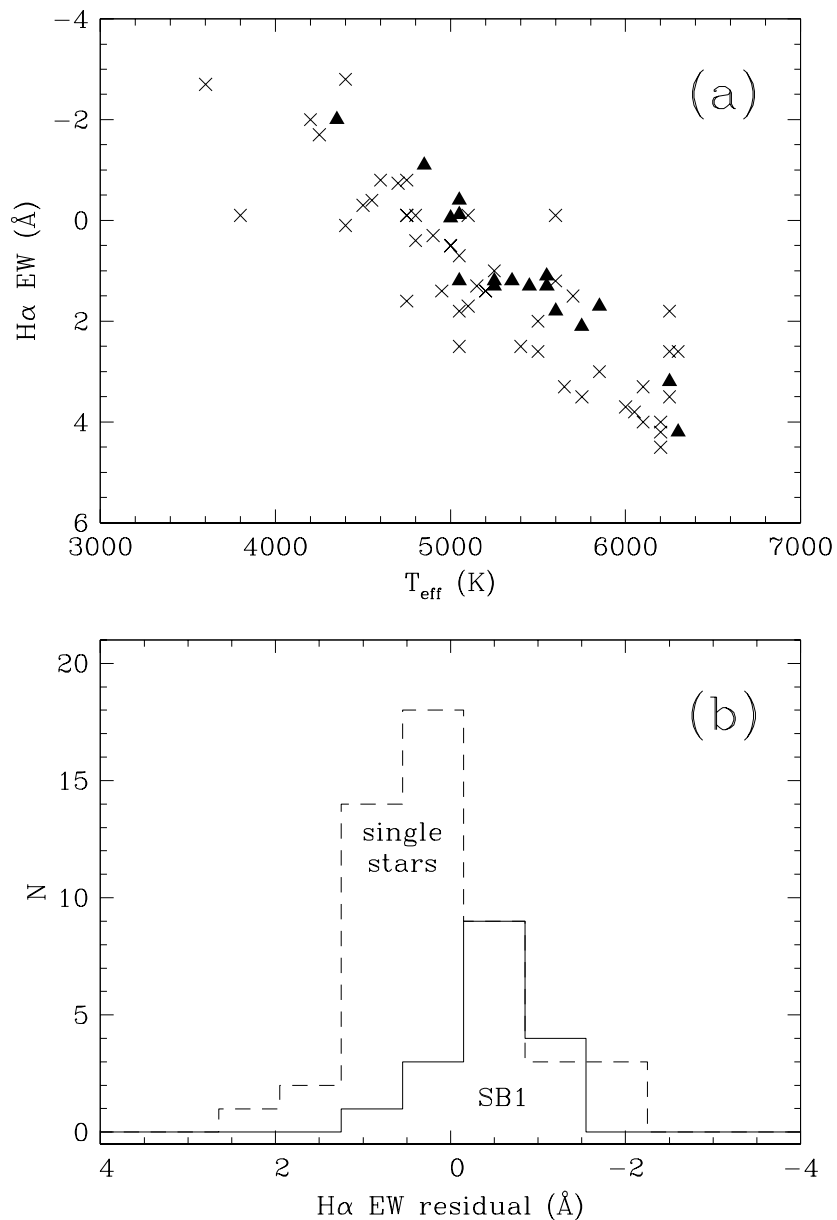


Fig. 9.— (a) H α equivalent width (\AA) as a function of the effective temperature, separately for the single-lined binaries in the present sample (triangles) and the single stars in N97 (crosses). Negative values indicate emission, and positive values represent absorption (partially filled-in or not). A similar correlation is seen for both kinds of objects. (b) Histogram of residuals from a linear fit to all points in (a), to highlight the fact that the binaries tend to have slightly stronger emission than the single stars (see text).

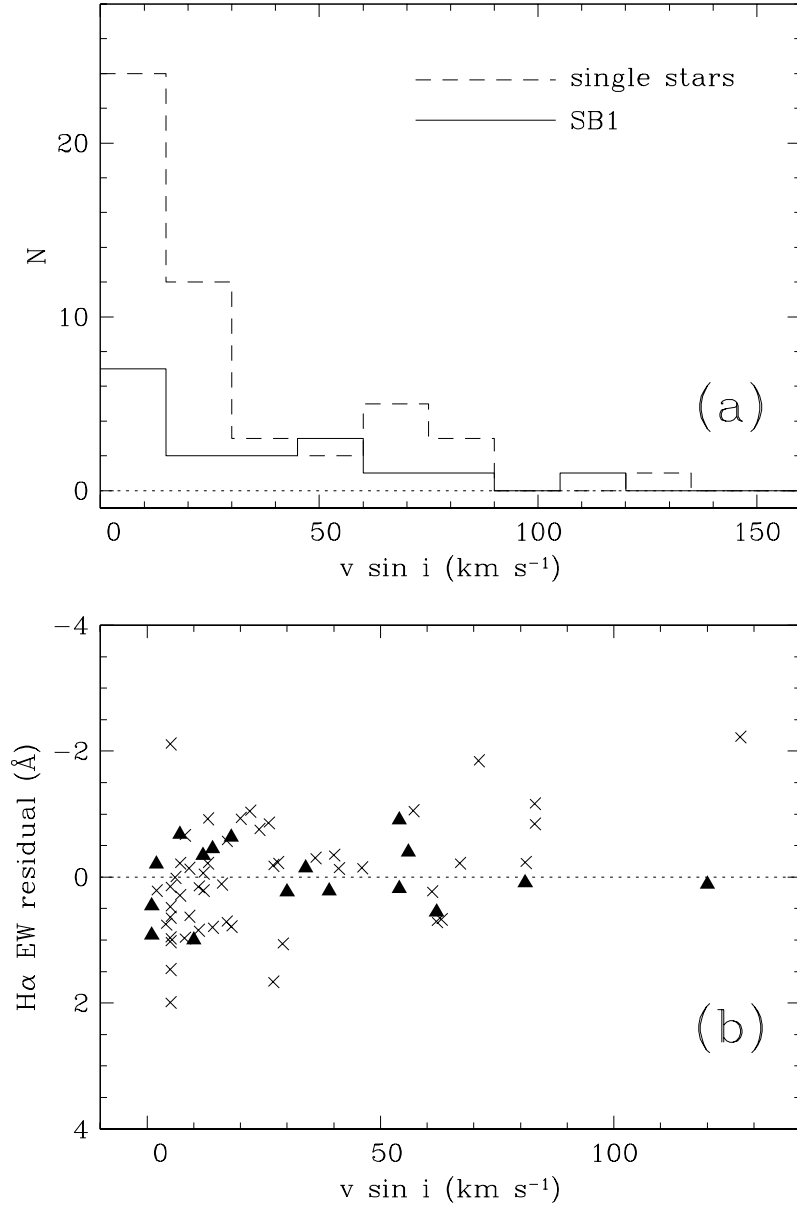


Fig. 10.— (a) Distribution of the projected rotational velocities for the single stars in N97 and for the single-lined binaries in our sample. No significant differences are seen. (b) Residuals from a linear fit to Figure 9a, corrected for the systematic offset shown in Figure 9b, separately for the SB1s and the single stars. Symbols as in Figure 9a.

TABLE 1. Main properties of the sample of binaries reported in this paper.

#	Star	R.A. (J2000)	Dec. (J2000)	V (mag)	SpT ^a	H α EW ^{a,b} (Å)	Li EW ^a (Å)	Li EW ^c (Å)
1	RXJ0209.1–1536	02:09:06.7	–15:35:43	13.00	dK4e	–1.2	no	
2	RXJ0210.4–1308SW	02:10:25.6	–13:07:56	12.5	dK3e	–0.12	no	
3	RXJ0212.3–1330	02:12:18.6	–13:30:41	11.40	K1	1.2	no	
4	RXJ0218.6–1004	02:18:39.5	–10:04:05	11.80	G8	1.6	no	
5	RXJ0219.7–1026	02:19:47.4	–10:25:40	11.60	K4	–0.25	0.1:	0.14,0.13
6	RXJ0239.1–1028	02:39:08.7	–10:27:44	13.20	dK7-M0e	–0.35	no	
7	RXJ0248.3–1117	02:48:22.2	–11:17:12	12.00	G7	2.1	no	
8	RXJ0251.8–0203	02:51:48.4	–02:03:38	12.70	dK6e	–0.60	no	0.06
9	RXJ0254.8–0709SE	02:54:52.4	–07:09:24	14.50	dM3e	–2.2	no	
10	RXJ0255.8–0750S	02:55:52.7	–07:50:39	14.00	K7-M0e	–0.2	no	no
11	RXJ0300.9–1002	03:00:54.2	–10:02:05	7.78	G0	no
12	RXJ0309.1+0324N	03:09:09.7	+03:23:44	10.22	F7	3.6	no	
13	RXJ0330.7+0306N	03:30:43.3	+03:05:48	10.89	dK5e	1.1f	no	
14	RXJ0339.6+0624	03:39:40.6	+06:24:44	11.30	G9	–0.1	0.13	
15	RXJ0340.3+1220	03:40:19.0	+12:20:18	12.47	dK5e	–1.1	no	
16	RXJ0343.6+1039	03:43:40.3	+10:39:14	10.20	K0	1.5	0.1	
17	RXJ0350.2+0849	03:50:12.9	+08:49:34	12.10	dK5e	–0.2	no	
18	RXJ0400.0+0730	04:00:01.0	+07:30:10	12.21	G3	1.3	no	
19	RXJ0402.5+0552	04:02:35.5	+05:51:35	10.81	G4	1.7	no	
20	RXJ0403.5+0837	04:03:29.5	+08:37:14	12.60	K0	1.3	no	
21	RXJ0405.5+0324	04:05:30.1	+03:23:50	11.47	dK4e	–0.4	no	
22	RXJ0408.6+1017	04:08:39.7	+10:17:32	12.62	G7	1.8	no	no
23	RXJ0410.6+0608	04:10:39.5	+06:08:39	12.94	K4	–0.05	0.11	
24	RXJ0422.9+0141	04:22:54.4	+01:41:31	12.27	F8	1.5	0.13+0.16	no+0.06
25	RXJ0427.8+0049	04:27:52.8	+00:49:26	9.98	G3	3.2	no	
26	RXJ0429.9+0155	04:29:56.8	+01:54:49	11.11	K3/K3III	1.5	no	
27	RXJ0434.3+0226	04:34:19.4	+02:26:26	12.32	K4	–0.4	0.3	0.20
28	RXJ0435.5+0455	04:35:31.4	+04:55:33	9.72	K3III	1.2	no	
29	RXJ0441.1+1132	04:41:07.4	+11:32:10	11.01	G0	
30	RXJ0441.9+0537	04:41:57.5	+05:36:34	9.57	G8+K1-2III ^d	var ^d	no	
31	RXJ0442.3+0118	04:42:18.4	+01:17:40	11.94	dK2e	–1.0	no	
32	RXJ0442.6+1018	04:42:40.6	+10:17:44	8.24	K3/K3III	1.2	no	
33	RXJ0442.9+0400	04:42:54.5	+04:00:11	10.94	K0	1.1	0.22	
34	RXJ0444.3+0941	04:44:20.3	+09:41:07	8.68	F9	3.2	no	
35	RXJ0444.4+0725	04:44:27.1	+07:24:59	13.67	K5	–0.3	0.12	
36	RXJ0451.6+0619	04:51:41.3	+06:19:21	12.76	dK2e	1.3f	no	
37	RXJ0503.6+1259	05:03:38.1	+12:59:45	13.05	
38	RXJ0515.3+1221	05:15:20.4	+12:21:14	11.58	dK0e	1.2f	no	
39	RXJ0523.0+0934	05:23:04.5	+09:34:01	10.39	F8	4.2	no	
40	RXJ0523.5+1005	05:23:33.5	+10:04:30	11.22	dK3e	–0.5	no	
41	RXJ0528.9+1046	05:28:58.3	+10:45:38	12.65	K3	0.1f	0.4	0.27+0.15
42	RXJ0529.3+1210	05:29:18.8	+12:09:30	12.86	K7-M0	–2.0	0.35	0.27
43	RXJ0530.9+1227	05:30:57.1	+12:27:27	10.68	K0	1.3	no	

^aSpectral types and equivalent widths from M97. A “no” for the Li EW means no line detected.

^bNegative values represent emission, and “f” means the line is filled-in compared to normal absorption for this spectral type.

^cEquivalent width measurements from this paper (#11, 22, 24, 27, 42) and other sources (#5 and 8 from N95; #5 and 10 from N97; #41 from Dolan & Mathieu 2001).

^dAdopted from Torres, Neuhäuser & Wichmann (1998).

Table 2. Measured (heliocentric) radial velocities for the single-lined binaries in the sample.

HJD (2,400,000+)	RV_A (km s^{-1})	$(O-C)_A$ (km s^{-1})	Orbital phase
[2] RXJ0210.4–1308SW (02:10:25.6 –13:07:56)			
49732.5746	53.93	–0.77	0.912
50033.7571	10.31	–2.10	0.271
50052.6145	–9.38	–3.36	0.655
50089.6196	–15.73	–0.56	0.391
50093.6267	28.60	–0.13	0.210

Note. — The complete version of this table is in the electronic edition of the Journal. The printed edition contains only a sample.

Table 3. Measured (heliocentric) radial velocities for the double-lined binaries in the sample.

HJD (2,400,000+)	RV_A (km s^{-1})	RV_B (km s^{-1})	$(O-C)_A$ (km s^{-1})	$(O-C)_B$ (km s^{-1})	Orbital phase
[1] RXJ0209.1–1536 (02:09:06.7 –15:35:43)					
49732.5908	16.13	27.62	–2.87	+13.52	0.590
49964.8905	87.30	–71.50	–2.80	–2.21	0.850
50002.8802	–8.99	56.00	+2.49	+6.15	0.519
50004.8241	90.37	–82.45	+0.54	–13.48	0.856
50033.7465	36.56	–4.19	+2.02	–0.07	0.625

Note. — The complete version of this table is in the electronic edition of the Journal. The printed edition contains only a sample.

TABLE 4. Effective temperature, surface gravity, and projected rotational velocity determinations for the single-lined binaries.

#	Star	T_{eff}^A (K)	$\log g_A$	$v_A \sin i$ (km s^{-1})
2	RXJ0210.4–1308SW	5050	4.5	56
7	RXJ0248.3–1117	5750	4.5	54
15	RXJ0340.3+1220	4850	4.5	54
19	RXJ0402.5+0552	5600	4.0	14
20	RXJ0403.5+0837	5550	4.0	34
22	RXJ0408.6+1017	5600	4.0	30
23	RXJ0410.6+0608	5000	4.5	2:
27	RXJ0434.3+0226	5050	4.0	7
28	RXJ0435.5+0455	5250	4.5	1:
32	RXJ0442.6+1018	5050	4.5	1:
33	RXJ0442.9+0400	5550	4.5	12
34	RXJ0444.3+0941	6250	4.5	120
36	RXJ0451.6+0619	5450	4.5	81
38	RXJ0515.3+1221	5350	4.5	10
39	RXJ0523.0+0934	6300	4.5	39
42	RXJ0529.3+1210	4350	4.0	18
43	RXJ0530.9+1227	5250	4.0	62

TABLE 5. Effective temperature, surface gravity, and projected rotational velocity determinations for the double-lined binaries.

#	Star	T_{eff}^A (K)	$\log g_A$	$v_A \sin i$ (km s^{-1})	T_{eff}^B (K)	$\log g_B$	$v_B \sin i$ (km s^{-1})	L_B/L_A (@5187 Å)
1	RXJ0209.1–1536	5200	4.5	41	4700:	4.5	35:	0.19
3	RXJ0212.3–1330	5050	4.5	7:	4450	4.5	5:	0.09
4	RXJ0218.6–1004	5050	3.5	26	6200	4.0	16	2.14
5	RXJ0219.7–1026	4800	3.0	32	5400	4.5	4:	0.06
6	RXJ0239.1–1028	4650	4.5	18	4500	4.5	16	0.36
8	RXJ0251.8–0203	4700	3.0	27	4650	3.0	24	0.71
9	RXJ0254.8–0709SE	3750:	4.5:	0:	3750:	4.5:	0:	0.19
10	RXJ0255.8–0750S	4600	4.5	8	4550	4.5	8:	0.68
11	RXJ0300.9–1002	5550	4.0	9	5400	4.0	7	0.55
12	RXJ0309.1+0324N	5800	4.0	118	5300:	4.0	95:	0.24
13	RXJ0330.7+0306N	5300	4.0	40	5400	4.5	28	0.63
14	RXJ0339.6+0624	4700	3.0	18	6000	4.5	3:	0.60
16	RXJ0343.6+1039	4800	3.5	20	6300	4.0	9	4.0
17	RXJ0350.2+0849	4750	3.5	49	5550	4.0	19	1.22
18	RXJ0400.0+0730	5700	3.5	33	7750:	4.5	0:	0.10
21	RXJ0405.5+0324	5000	4.0	16	6700	4.5	7:	1.11
24	RXJ0422.9+0141	4550	3.0	37	6300	4.0	14	4.1
25	RXJ0427.8+0049	5900	4.0	24	5950	4.0	17	0.67
26	RXJ0429.9+0155	5350	4.5	8	5250	4.5	0:	0.24
29	RXJ0441.1+1132	5300	4.5	18	4750:	4.5	0:	0.07
30	RXJ0441.9+0537 ^a	4960	3.0	22	4530	2.0	31	1.06
31	RXJ0442.3+0118	4850	3.5	24	5200	4.5	5:	0.16
35	RXJ0444.4+0725	4950	4.5	20	4650:	4.5	15:	0.13
37	RXJ0503.6+1259	4600	3.0	29	4500:	4.5:	0:	0.07
40	RXJ0523.5+1005	5500	4.5	51	5250	4.5	38	0.22
41	RXJ0528.9+1046	4800	3.5	10	4550	3.5	9	0.34

^aResults for this system are adopted from Torres, Neuhäuser & Wichmann (1998).

TABLE 6. Orbital solutions for the single-lined binaries.

#	Star	P (days)	γ (km s^{-1})	K_A (km s^{-1})	e	ω (deg)	T^a (HJD-2,400,000)	$M_B \sin i^b$ (M_\odot)	$a_A \sin i$ (10^6 km)	Span N	σ (km s^{-1})
2	RXJ0210.4-1308SW	0.6886391	+18.14	42.9	0	...	50399.2377	0.178	0.406	1096	2.67
		0.0000095	0.76	1.0	0.0042	0.029	0.066	14	
7	RXJ0248.3-1117	1.0072701	+7.44	74.48	0	...	50249.6386	0.351	1.032	1388	2.13
		0.0000051	0.56	0.75	0.0016	0.018	0.052	18	
15	RXJ0340.3+1220	0.5548876	+16.7	40.5	0	...	50250.7563	0.156	0.309	1217	3.77
		0.0000056	1.0	1.3	0.0031	0.044	0.086	19	
19	RXJ0402.5+0552	8.18561	+35.72	25.79	0.029	287.	50309.40	0.2440	2.901	1144	0.67
		0.00032	0.19	0.27	0.010	21.	0.48	0.0034	0.041	16	
20	RXJ0403.5+0837	2.157175	-3.48	41.91	0	...	50320.6656	0.2543	1.243	1214	1.32
		0.000026	0.36	0.44	0.0047	0.0085	0.041	16	
22	RXJ0408.6+1017	2.388939	-34.16	53.32	0	...	50356.7373	0.3348	1.751	1215	0.75
		0.000017	0.23	0.30	0.0023	0.0036	0.019	13	
23	RXJ0410.6+0608	16.05305	-1.27	19.47	0.2234	288.1	50520.376	0.2248	4.189	1172	0.39
		0.00070	0.12	0.14	0.0078	2.3	0.090	0.0014	0.025	14	
27	RXJ0434.3+0226	603.3	+23.32	7.13	0.360	54.4	50477.1	0.2641	55.2	1916	0.53
		3.7	0.18	0.22	0.032	5.3	7.1	0.0075	1.6	15	
28	RXJ0435.5+0455	40.950	+4.34	13.39	0.403	71.7	49923.93	0.1984	6.90	887	0.59
		0.033	0.14	0.25	0.016	2.7	0.28	0.0034	0.12	21	
32	RXJ0442.6+1018	26.9130	+47.195	17.11	0.3569	185.1	50121.079	0.2250	5.916	1118	0.35
		0.0046	0.089	0.16	0.0065	1.3	0.085	0.0013	0.034	21	
33	RXJ0442.9+0400	509.8	+22.39	8.90	0.093	115.	50474.	0.332	62.1	1895	0.64
		1.6	0.23	0.30	0.025	24.	32.	0.015	2.7	16	
34	RXJ0444.3+0941	0.6854791	+28.5	57.8	0	...	50127.9384	0.240	0.55	1404	4.95
		0.0000042	1.2	1.7	0.0031	0.077	0.18	21	
36	RXJ0451.6+0619	0.6975758	-26.5	130.9	0	...	50317.4658	0.545	1.26	1181	4.02
		0.0000025	1.1	1.3	0.0016	0.054	0.12	16	
38	RXJ0515.3+1221	63.135	+62.50	24.07	0.343	293.1	50858.84	0.423	19.6	1890	1.85
		0.016	0.29	0.49	0.015	3.7	0.54	0.029	1.4	46	
39	RXJ0523.0+0934	1.470169	-34.24	35.09	0	...	50275.8907	0.187	0.709	1399	1.94
		0.000023	0.57	0.78	0.0048	0.020	0.076	14	
42	RXJ0529.3+1210	462.78	+18.71	24.4	0.910	104.	51034.6	0.368	65.	2362	1.88
		0.67	0.68	6.3	0.055	12.	3.7	0.065	11.	34	
43	RXJ0530.9+1227	1.483685	+92.44	36.20	0	...	50417.9177	0.194	0.74	2097	3.11
		0.000016	0.67	0.91	0.0064	0.034	0.13	23	

^aFor eccentric orbits this is the time of periastron passage, and for circular orbits it is the time of maximum primary velocity.

^bListed in this column is the coefficient $f^{1/3}$ in the expression $M_B \sin i = f^{1/3}(M_A + M_B)^{2/3}$ for the minimum mass of the secondary component.

TABLE 7. Orbital solutions for the double-lined binaries.

#	Star	P (days)	γ (km s^{-1})	K_A (km s^{-1})	K_B (km s^{-1})	e	ω (deg)	T^a (HJD-2,400,000)	q (M_B/M_A)	$a \sin i$ (R_\odot)	$M_A \sin^3 i$ (M_\odot)	$M_B \sin^3 i$ (M_\odot)	Span N	σ_A σ_B
1	RXJ0209.1-1536	0.8318408	+16.74	72.88	85.5	0.0184	60.	50183.790	0.853	2.602	0.185	0.1574	1325	1.95
		0.0000049	0.46	0.70	3.3	0.0090	33.	0.077	0.037	0.061	0.016	0.0079	18	9.50
3	RXJ0212.3-1330	6.709914	+34.191	55.45	68.9	0	...	50183.8292	0.804	16.49	0.741	0.596	766	0.38
		0.000076	0.087	0.11	1.1			0.0026	0.014	0.16	0.027	0.012	20	3.81
4	RXJ0218.6-1004	5.787321	+3.76	72.56	74.59	0.0069	314.	50116.42	0.9728	16.824	0.9683	0.942	708	1.29
		0.000095	0.13	0.38	0.17	0.0028	19.	0.31	0.0061	0.053	0.0074	0.011	19	0.59
5	RXJ0219.7-1026	8.11944	-6.21	44.02	80.89	0	...	50401.102	0.5442	20.04	1.062	0.578	1326	1.25
		0.00033	0.26	0.33	0.88			0.012	0.0077	0.16	0.029	0.012	22	3.39
6	RXJ0239.1-1028	2.0720160	-11.73	90.70	95.99	0.0093	67.	50537.20	0.945	7.642	0.718	0.679	2213	1.51
		0.000063	0.29	0.47	0.93	0.0048	31.	0.18	0.011	0.046	0.016	0.016	25	3.28
8	RXJ0251.8-0203	8.01303	-12.07	56.37	57.16	0	...	50359.4927	0.986	17.97	0.612	0.603	1325	1.79
		0.00020	0.32	0.54	0.94			0.0092	0.020	0.18	0.022	0.016	26	3.15
9	RXJ0254.8-0709SE	11.79507	+24.67	24.58	42.6	0	...	50509.942	0.577	15.66	0.235	0.1357	1419	0.77
		0.00064	0.20	0.28	1.6			0.022	0.024	0.42	0.022	0.0078	16	4.77
10	RXJ0255.8-0750S	3.701806	+15.78	71.05	73.34	0	...	50179.5312	0.9687	10.560	0.5864	0.5681	1009	0.89
		0.000019	0.15	0.38	0.30			0.0015	0.0072	0.039	0.0064	0.0072	14	0.69
11	RXJ0300.9-1002	5.502945	-8.486	50.39	52.91	0	...	51223.0191	0.9523	11.231	0.3220	0.3066	703	0.41
		0.000071	0.070	0.12	0.18			0.0018	0.0041	0.025	0.0024	0.0019	26	0.64
12	RXJ0309.1+0324N	0.45504147	+9.1	84.6	155.4	0	...	50747.6203	0.544	2.158	0.422	0.230	2194	7.41
		0.0000084	1.4	2.0	4.7			0.0015	0.022	0.048	0.032	0.014	25	17.52
13	RXJ0330.7+0306N	1.3639071	+22.10	82.65	88.91	0	...	50068.5079	0.930	4.623	0.3698	0.3438	884	2.08
		0.000062	0.34	0.67	0.94			0.0011	0.013	0.033	0.0090	0.0070	26	2.98
14	RXJ0339.6+0624	5.11620	+45.31	20.20	22.92	0	...	50495.8051	0.881	4.358	0.02259	0.01990	1388	1.11
		0.00014	0.17	0.31	0.37			0.0094	0.021	0.052	0.00086	0.00073	25	1.31
16	RXJ0343.6+1039	4.738720	-43.51	37.25	38.94	0	...	50023.3580	0.957	7.134	0.1110	0.1062	1133	2.31
		0.000059	0.12	0.64	0.20			0.0031	0.018	0.066	0.0023	0.0038	31	0.69
17	RXJ0350.2+0849	3.159378	-6.30	70.4	76.78	0	...	50428.5119	0.916	9.184	0.544	0.499	1454	4.85
		0.000030	0.31	1.3	0.33			0.0035	0.019	0.089	0.011	0.019	21	1.17
18	RXJ0400.0+0730	4.67647	-28.76	59.49	87.4	0	...	50213.944	0.680	13.57	0.914	0.622	1477	1.59
		0.00012	0.48	0.53	2.6			0.010	0.023	0.27	0.066	0.027	16	8.45
21	RXJ0405.5+40324	14.22909	-23.06	38.37	48.13	0.0102	40.	49926.8	0.7972	24.32	0.5310	0.4233	1507	1.10
		0.00069	0.15	0.31	0.28	0.0048	27.	1.1	0.0084	0.13	0.0082	0.0076	26	0.99
24	RXJ0422.9+0141	5.36761	+7.03	72.3	76.69	0	...	50560.8645	0.943	15.80	0.947	0.893	1504	5.01
		0.00011	0.30	1.7	0.47			0.0068	0.025	0.21	0.028	0.047	16	1.24
25	RXJ0427.8+0049	4.238794	-20.95	79.80	81.47	0	...	49845.2984	0.9795	13.506	0.9307	0.9116	1411	1.06
		0.000025	0.13	0.27	0.22			0.0016	0.0044	0.031	0.0062	0.0069	28	0.86
26	RXJ0429.9+0155	89.579	-11.23	30.34	32.21	0.1434	235.4	50220.68	0.942	109.6	1.134	1.068	1181	0.67
		0.030	0.18	0.34	0.85	0.0068	3.7	0.93	0.029	1.8	0.069	0.043	21	2.20
29	RXJ0441.1+1132	2.548348	-16.35	73.42	97.8	0.0126	324.	50016.02	0.751	8.62	0.756	0.568	764	0.83
		0.000016	0.26	0.44	2.1	0.0049	17.	0.12	0.018	0.12	0.039	0.017	19	6.23
31	RXJ0442.3+0118	8.75655	+1.67	49.67	76.0	0	...	50613.531	0.653	21.75	1.090	0.712	2151	1.61
		0.00024	0.31	0.40	1.1			0.014	0.012	0.22	0.038	0.017	24	4.46
35	RXJ0444.4+0725	1.994974	+9.69	73.2	98.2	0	...	50837.2813	0.746	6.76	0.597	0.445	2301	1.61
		0.000016	0.41	1.4	3.1			0.0035	0.023	0.17	0.050	0.030	15	6.06
37	RXJ0503.6+1259	2.339866	+23.60	16.00	33.4	0.199	173.8	50788.611	0.479	2.238	0.01861	0.00891	2300	1.96
		0.000041	0.41	0.66	1.0	0.028	7.8	0.046	0.026	0.068	0.00173	0.00086	17	2.99
40	RXJ0523.5+1005	0.5461672	-17.85	63.78	76.2	0	...	50444.3303	0.837	1.510	0.0845	0.0707	1775	2.12
		0.000015	0.60	0.69	2.1			0.0015	0.027	0.025	0.0052	0.0027	17	7.24
41	RXJ0528.9+1046	7.67246	+28.29	42.72	45.00	0.0290	260.	50278.88	0.949	13.29	0.2749	0.2610	1125	0.85
		0.00018	0.18	0.32	0.57	0.0071	12.	0.26	0.015	0.11	0.0082	0.0058	21	1.64

^aFor eccentric orbits this is the time of periastron passage, and for circular orbits it is the time of maximum primary velocity.